Title
Mechanisms Mediating Development of Refinement of Retinogeniculate Connections

Author
Koch, Selina Marie

Publication Date
2011

Peer reviewed|Thesis/dissertation

Mechanisms Mediating Development and Refinement of Retinogeniculate Connections

by

Selina Koch

DISSERTATION

Submitted in partial satisfaction of the requirements for the degree of

DOCTOR OF PHILOSOPHY

in

Neuroscience

in the

GRADUATE DIVISION

of the

UNIVERSITY OF CALIFORNIA, SAN FRANCISCO

Dedications and Acknowledgements

I wish to acknowledge the intellectual and technical support of my thesis advisor Dr. Erik Ullian, the assistance of my collaborators Dr. Andrew Huberman, Cassandra Dela Cruz, Dr. Thomas Hnasko, and Robert Edwards, M.D., and the thoughtful comments made by my thesis committee Dr. David Copenhagen, Dr. Michael Stryker, Dr. Herwig Baier, and Dr. Marla Feller.

I acknowledge that the text in Chapter 2 of this dissertation is a reprint of the material as it will appear in Neuron: Koch, S.M., Dela Cruz C.G., Hnasko, T.S., Edward, R.H., Huberman, A.D., Ullian E.M. (2011) Pathway-specific genetic attenuation of glutamate release alters select features of competition-based visual circuit refinement. In press. I acknowledge that Thomas Hnasko and Robert Edwards made the conditional VGluT2 knockout mice that were used in the study. Cassandra Dela Cruz performed the immunostaining experiment shown in Figure 2.3. Andrew Huberman provided intellectual input and assisted in writing and editing the manuscript. Erik Ullian directed and supervised the research.

I acknowledge that the text in Chapter 3 of this dissertation is a reprint of the material as it appears in the Journal of Neuroscience: Koch, S.M. and Ullian, E.M. (2010) Neuronal pentraxins mediate silent synapse conversion in the developing visual system. J Neurosci *30,* 5404-5414. The coauthor listed in the publication, Erik Ullian, directed and supervised the research that forms the basis for both chapters 2 and 3 of this dissertation.

Abstract

A hallmark of mammalian neural circuit development is the refinement of initially imprecise connections through activity-dependent competition. A prime example of this takes place in the developing visual system where retinal ganglion cell (RGC) axons from the two eyes compete for territory in the dorsal lateral geniculate nucleus (dLGN). Despite numerous experiments indicating that spontaneous spiking activity in the retina drive eye-specific axonal competition, the direct contributions made by synaptic transmission to eye-specific refinement remain unclear. Chapter 2 of this manuscript attempts to narrow this gap. In that study a novel mouse genetic strategy was used to disrupt glutamate release from a defined population of RGCs, the ipsilateral-projecting RGCs. We found that when glutamate release from ipsilateral-RGC axons is reduced, they fail to exclude competing contralateral axons from their target region in the dLGN. Nevertheless, the release-deficient axons both consolidated and maintained their normal amount of dLGN territory in the face of fully active, competing axons. These data demonstrate that during visual circuit refinement glutamate-based competition plays a direct role in removing axons from inappropriate target regions, and they argue that axonal consolidation within appropriate target regions is largely insensitive to synaptic competition. Chapter 3 investigates the roles of two proteins, neuronal pentraxins 1 and 2 (NP1/2), during retinogeniculate development. NP1/2 are hypothesized to play important roles in the development of AMPAR-mediated synaptic transmission and their absence disrupts eye-specific refinement; therefore we hypothesized that NP1/2 might participate in the synaptic mechanisms that refine eye-specific RGC-dLGN projections. Electrophysiological analysis was performed on thalamic slices from mice lacking NP1/2, which showed a specific reduction in AMPAR-mediated synaptic transmission during the period when eye-specific territories form. This was the first demonstration that NP1/2 are required *in vivo* for the normal development of AMPAR-mediated synaptic transmission and is consistent with a role for NP1/2 in mediating eye-specific refinement through synaptic mechanisms. The basis of the reduced AMPAR currents and their relationship to the structural defects exhibited by NP1/2 KO

RGC axons were further explored. Chapter 4 discusses the findings from the two studies and suggests additional experiments that could extend the present findings.

Table of contents

Chapter 1 — Introduction

1.1 Organization of retinal projections in the visual thalamus

1.2 Emergence of exclusive eye-specific axonal territories in the dLGN

Figure 1. Refinement of RGC axons in the mouse dLGN.

1.3 Molecular mechanisms that refine RGC-dLGN connections

1.4 Activity-dependence of eye-specific axon segregation

1.5 Does retinal activity instruct eye-specific refinement?

1.6 Synaptic mechanisms implicated in eye-specific segregation

1.7 What lies ahead

Chapter 2 — Pathway-specific genetic attenuation of glutamate release alters select features of competition-based visual circuit refinement

2.1 Results

2.1.1 A genetic approach to selectively alter gene expression in ipsilateral-projecting RGCs

Figure2.1 A transgenic mouse that expresses Cre selectively in ipsilateral-projecting RGCs.

Figure 2.2 Cre-driven reporter expression in ET33 Sert-Cre mice is restricted to ipsilateral-projecting RGCs and initiates embryonically.

2.1.2 Pathway specific attenuation of vesicular glutamate release

Figure 2.3 Loss of VGluT2 immunoreactivity in cultured RGCs taken from ET33-Cre::VGluT2$^{flox/flox}$ animals.

Figure 2.4 ET33-Cre driven removal of VGlut2 reduces NMDAR-mediated synaptic currents in the ipsilateral RGC-dLGN pathway.

Figure 2.5 ET33-Cre driven VGlut2 removal reduces AMPAR-mediated synaptic currents in the ipsilateral retinogeniculate pathway.

2.1.3 Attenuation of glutamatergic transmission impacts select aspects of retinogeniculate refinement

Figure 2.6 Reduced ipsilateral synaptic transmission perturbs eye-specific axonal refinement but does not prevent the establishment of ipsi-eye territory in the dLGN.

Figure 2.7 Ipsilateral RGC axons exhibit normal territory consolidation despite severely impaired synaptic glutamate release.

Figure 2.8 VGluT2-deficient ipsi-RGC axons are constrained by glutamate releasing contra-RGC axons.

Figure 2.9 Maintenance of ipsilateral retinogeniculate axonal projections in the face of prolonged disruption of glutamatergic synaptic transmission.

Figure 2.10 ET33-Cre::VGluT2$^{flox/flox}$ results compared to studies in which retinal waves were manipulated.

2.2 Discussion

2.3 Materials and Methods

Chapter 3 — Neuronal pentraxins mediate silent synapse conversion in the developing visual system

3.1 Introduction

3.2 Results

Figure 3.1 NP1/2 knockout neurons have a specific deficit in AMPAR-mediated synaptic transmission during early postnatal development (P6-P9).

Figure 3.2 Increased retinal activity *in vivo* over multiple days (P5-P7/ 8) does not lead to reduced retinogeniculate transmission.

Figure 3.3 Quantal size is not reduced in early postnatal NP1/2 KO dLGN neurons (P6-P9).

Figure 3.4 Young NP1/2 KO dLGN neurons (P6-P9) have an increased number of silent synapses.

Figure 3.5 P17-P20 NP1/2 KO animals strengthen AMPAR-mediated currents by an NP1/2-independent mechanism and develop aberrantly large current amplitudes.

Figure 3.6 NP1/2 KOs display abnormal input elimination during development.

Figure 3.7 Monocular epibatidine treatment from P4 to P10 fails to drive axon remodeling in NP1/2 KOs.

3.3 Discussion

3.3.1 NP1/2 loss leads to reduced synaptic AMPAR-mediated currents in vivo

3.3.2 Are the affects of NP1/2 on retinogeniculate transmission direct?

3.3.3 The requirement for NP1/2 is restricted to a specific developmental period

3.3.4 What is the basis of the excessive synaptic currents observed in the P17-P20 NP1/2 knockout animals?

3.3.5 What accounts for the eye-specific segregation defects in NP1/2 KOs?

3.4 Material and Methods

Chapter 4 — Discussion

4.1 What is the role of glutamatergic synaptic transmission in eye-specific refinement?

4.2 What is the glutamate-dependent mechanism that eliminates mis-targeted axons?

4.3 Does glutamatergic synaptic transmission stabilize developing RGC axons?

4.4 Summary

References Section

Chapter 1 — Introduction

Precisely tuned neural circuits are the substrate for cognition, perception and behavior. To date, much remains unknown about the developmental mechanisms that establish precise CNS circuits. While patterned spontaneous activity in immature circuits helps to refine their connectivity (Blankenship and Feller, 2010; Huberman et al., 2008a), the direct contributions of synaptic transmission to circuit refinement are largely undefined. The experiments presented in the following chapters use a longstanding model for investigating activity mediated CNS circuit refinement - the refinement of retinal inputs to the visual thalamus - to gain new insight into the direct roles played by glutamatergic synaptic transmission in sculpting precise CNS circuits.

1.1 Organization of retinal projections in the visual thalamus

The dorsal lateral geniculate nucleus of the thalamus (dLGN) is the gateway through which visual information is transmitted from the retina to the cortex; therefore, visual perception relies on the ability of dLGN neurons to faithfully relay the specific features of the visual world encoded by the retina. Accordingly, the connections between retinal ganglion cells (RGCs) and dLGN neurons are highly organized (Kaas et al., 1972; Rodieck, 1979). For instance, RGC projections are arranged such that neighboring cells in the retina innervate neighboring cells in the dLGN creating a retinotopic map in the dLGN. In fact, the dLGN contains multiple, overlaid visual maps since several functionally-distinct subtypes of RGCs populate the retina and each subtype samples the entire visual scene (or a large portion of it) by tiling the retinal surface in a mosaic fashion (Wassle, 2004). Cell-type-specific organization exists in the dLGN as well since different types of dLGN neurons reside in distinct dLGN laminae and receive input from subsets of RGCs (Rodieck, 1979; Leventhal et al., 1981; Leventhal et al., 1985) (functional input layers have recently been shown in the mouse dLGN as well, Huberman et al., 2008b; Huberman, 2009; Kim et al., 2008; Kim et al., 2010). Another key feature of retinogeniculate organization which is important for binocular vision, and which is the focus of the experiments in chapters 2 and 3, is that the axons from the two eyes segregate

into distinct dLGN territories (Kaas et al., 1972). Thus, the signals arising from the left and right eyes remain separate at the level of the dLGN.

1.2 Emergence of exclusive eye-specific axonal territories in the dLGN

Throughout the mammalian nervous system many neural circuits transition from an unrefined state to a refined state in order to achieve their mature patterns of connections. Likewise, when RGC axons from the two eyes initially invade the dLGN they overlap extensively and only later segregate into non-overlapping territories (Godement et al., 1984; Linden et al., 1981; Rakic, 1976; Shatz, 1983). Eye-specific segregation has been observed in all mammals that have been examined. In humans, eye-specific territories form in utero during the second trimester (Hevner, 2000). In cats they form in the final few weeks of gestation (Shatz, 1983). In rodents, however, eye-specific refinement occurs postnatally (Godement, 1984), a fact that has made the rodent dLGN an attractive model for studies of mammalian RGC axon refinement. In mice, eye-specific segregation in the dLGN begins around postnatal day 4 (P4) and is largely completed by P10 (Godement, 1984; Juabert-Miazza, 2005; Ziburkus and Guido; 2006). On P4 contralateral-eye projections are present throughout the entire dLGN and are therefore completely overlapped with the ipsilateral projection, which is also large and diffuse at that age. Eye-specific dLGN layers are visible by P10. By this age the ipsilateral-RGC axons form a small, dense termination zone in the dorsal medial dLGN, which the contralateral-RGC axons evacuate (see Figure 1A-B for diagram).

Eye-specific segregation involves the pruning of inappropriately targeted axonal branches and the continued growth and branching of appropriately targeted branches (as opposed to, for instance, the rearrangement of existing axons). The morphological changes in individual RGC axons during eye-specific segregation were first characterized in cats by Sretavan and Shatz (1986) who showed that prior to eye-specific segregation individual RGC axons initially formed many side branches along their course through the dLGN with little regard for future eye-specific borders. As segregation proceeded side branches were eliminated from the opposite eye's territory and branching within the appropriate eye-specific

layer became denser. Similar findings were recently reported in the mouse dLGN (see Figure 1C-D and Dhande et al., 2011).

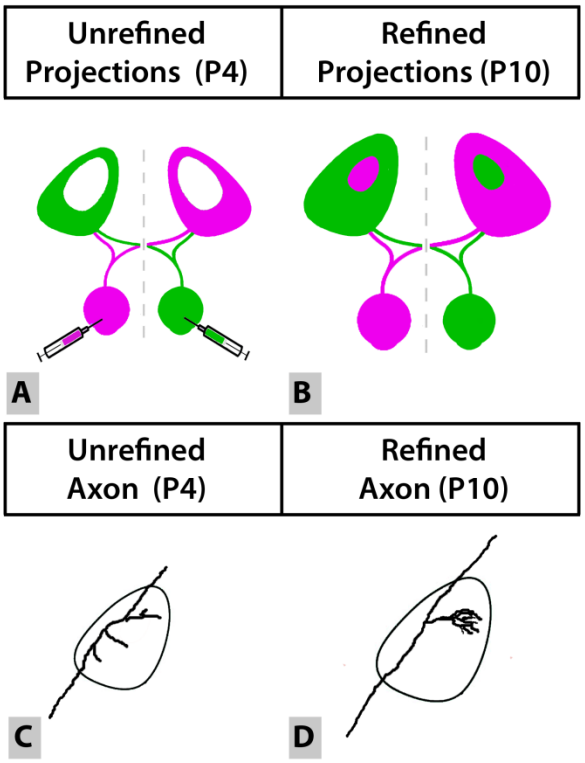

Figure 1. Refinement of RGC axons in the mouse dLGN. (A-B) Show bulk labeling of left and right eye RGC axons by intraocular injections of anterograde tracers. (A) RGC-dLGN projections in mice at age P4. White indicates region of overlap. (B) Eye-specific territories are clearly visible by P10. (C) Diagram shows a single unrefined RGC axon on P4. Axon contains multiple but sparse branches throughout the dLGN. (D) A single RGC axon on P10. The remaining branch is more elaborate and terminates in a focal region.

Eye-specific refinement is also accompanied by the formation and elimination of synapses. In the cat dLGN electron microscopic examination of RGC axons showed that many of their side branches formed structural synapses regardless of whether they were located in the appropriate eye-specific region (Campbell and Shatz, 1992), indicating that the removal of axonal improperly targeted axonal branches must also involve synapse elimination. This idea is supported by electrophysiological studies in cats and rodents which showed that prior to eye-specific segregation individual dLGN neurons receive weak synaptic inputs from several RGCs located in both eyes, whereas in adulthood dLGN neurons are monocularly driven, typically by strong connections from 1 to 3 RGCs (Mooney et al., 1996; Chen and Regehr, 2000; Ziburkus and Guido, 2006).

Thus, eye-specific refinement involves the elimination of inappropriate synaptic connections and the axonal branches on which they reside, as well as the continued growth of appropriately targeted axonal arbors.

1.3 Molecular mechanisms that refine RGC-dLGN connections

How do RGC axons and dLGN neurons decide which among their many initial contacts will be their permanent synaptic partners? It has become clear that multiple mechanisms influence these decisions, some of which are activity-mediated whereas others act largely independently from neural activity (Huberman, 2008a).

Among the molecular mechanisms that contribute to retinogeniculate patterning, the roles played by Eph/ephrin signaling have been the most thoroughly described. Interactions between Eph receptors and their ephrin ligands are chemorepellent, and gradients of Ephs and ephrins are present in both the retina and dLGN (reviewed in McLaughlin and O'Leary, 2005). Eph/ephrin gradients, therefore, carry positional information, and many studies indicate Eph/ephrin gradients set up retinotopy in the dLGN, and several studies have demonstrated that Eph/ephrin signaling mediates retinotopic map formation (McLaughlin and O'Leary, 2005; Huberman et al., 2008a).

Could the molecular guidance mechanisms that establish retinotopy also segregate the axons from the two eyes? This is an attractive hypothesis considering that the population of RGCs that project to the ipsilaterally reside in a particular location in the retina; namely, in the periphery of the ventral and temporal quadrants (Drager and Olsen, 1980; Dreher et al., 1985; Farid Ahmed et al., 1998; Herrera et al., 2003). The idea that the sorting of left and right eye axons could simply be the result of retinotopic map formation has been tested by over-expression of EphAs and knockout of ephrinAs. Over-expression of EphAs in ferret RGCs led to eye-specific targeting defects in the dLGN (Huberman et al., 2005), and triple knock-out of ephrinA2, A3, and A5 in mice led to abnormal fracturing and localization of eye-specific dLGN territories (Pfeiffenberger et al., 2005). While it is clear that the positions and shapes of

the eye-specific dLGN territories are critically dependent on EphA/ephrinA-mediated mapping mechanisms, those cues alone did not account for the segregation of eye-specific axonal projections. For instance, in the triple knock-out study mentioned above ipsi-eye and contra-eye axons still segregated from each other despite the observed abnormalities in the overall shape and position of the ipsi-occupied region (Pfeiffenberger et al., 2005). Segregation in the triple knock outs was abolished by activity blockade. Thus, Eph/ephrin signaling and neural activity influence distinct aspects of eye-specific refinement.

EphAs and ephrinAs are not the only molecules that have been implicated in RGC axon targeting. Other potential contributors include: EphBs/ephrinBs and Wnt/ryk signaling, which contribute to the patterning of the dorsal-ventral axis of the retina (reviewed in Salinas and Zou, 2008), engrailed 2, which can attract nasal RGCs and repel temporal RGCs (Brunet et al., 2005), and ten_m3, which limits the ventrolateral extent of ipsilateral axons in the dLGN (Leamey et al., 2007). Additional patterning molecules may continue to be identified, as well as the molecular pathways downstream of patterning signals and potential points of interaction between genetic programs and activity-dependent mechanisms. The experiments in this dissertation are, however, focused on the activity dependent mechanisms that sort RGC axons.

1.4 Activity-dependence of eye-specific axon segregation

Throughout the developing nervous system, activity in nascent neural circuits often affects the refinement of circuit connections through competitive mechanisms in which stronger more active connections are maintained and weaker less active connections are eliminated (Katz and Shatz, 1996; Sanes and Lichtman, 1999). Likewise, in the dLGN, eye-specific segregation involves competition between left and right eye axons that is mediated by spontaneous retinal activity. Competition between left and right eye axons was demonstrated by Rakic (1981) who showed that when one eye was removed after birth the axons arising from the remaining eye expanded to occupy greater dLGN territory, which suggested that the axons from one eye are normally constrained by the axons from the opposite eye. The activity-dependence of eye-specific refinement was first demonstrated by Shatz and Stryker (1988) who

showed that axonal segregation could be prevented by intracranial application of tetrodotoxin (ttx) near the optic tract. A variety of pharmacologic and genetic manipulations have since been used to disrupt retinal activity and have confirmed that spontaneous activity in the retina is critical for segregating RGC axons in the dLGN (Huberman et al., 2002; Huberman et al., 2003; Muir-Robinson et al., 2002; Penn et al., 1998; Rossi et al., 2001; but see Cook et al., 1999). A link between competition and activity was demonstrated in two pharmacological studies in which activity was either increased or decreased in just one eye (Penn et al., 1998; Stellwagen and Shatz, 2002). In both studies, the axons arising from the less active eye lost territory to the axons from the more active eye, suggesting that left and right eye axons compete through their relative synaptic efficacies. I address that hypothesis experimentally in Chapter 2.

1.5 Does retinal activity instruct eye-specific refinement?

Retinal activity is clearly required for eye-specific refinement and relative activity levels matter, but do particular features of retinal activity carry instructive signals for segregating RGC axons? This fundamental question has received considerable attention from researchers in the field, yet continues to generate controversy (Feller, 2009; Chalupa, 2009). To address this question this section will examine data regarding the structure of early spontaneous retinal activity and will explore which (if any) of its spatiotemporal features are required for normal eye-specific refinement.

Visual circuit refinement requires activity, yet it occurs before the onset of vision. It has become increasingly apparent that many developing neural circuits- including the retina, cochlea, hippocampus, spinal cord, and cerebellum- generate spontaneous activity patterns prior to the establishment of their adult-like connectivity and function (reviewed by Blankenship and Feller, 2010). Among the different brain regions that exhibit early spontaneous network activity, retinal activity patterns and their roles in visual circuit development have been most extensively studied.

The pattern of early spontaneous retinal activity has been investigated primarily through multi-electrode array recordings and calcium imaging experiments (reviewed in Huberman et al., 2008a). These studies have demonstrated that the properties of spontaneous retinal activity and the mechanisms that generate it change considerably over development and can be generally grouped into three developmental stages (stages I-III) (Bansal et al., 2000; Syed et al., 2004; Feller et al., 1996; Zheng et al., 2004; Wong et al., 2000; Zhou and Zhao, 2000). The bulk of eye-specific segregation happens during stage II (P1-P10) (Godement, 1984), which consists of periodic bursts of action potentials (and calcium transients) that propagate over large portions of the retina and are commonly referred to as "retinal waves" (Meister et al., 1991; Wong et al., 1995). Stage II retinal waves are triggered by transient cholinergic inputs onto RGCs from a class of interneurons called starburst amacrine cells, and propagate via the horizontal connections between the starburst cells and their connections to RGCs (Feller et al., 1996). During stage II waves individual RGCs fire bursts of action potentials roughly every 1.5 minutes with little spiking exhibited between bursts (Bansal et al., 2000; Feller et al., 1996; Stafford et al., 2009). RGCs within a wavefront fire in a temporally correlated fashion. Correlation strengths diminish as a function of distance between pairs of RGCs with adjacent RGCs exhibiting the strongest correlations and little to no correlations exhibited between RGCs separated by more than 500 microns (Stafford et al., 2009). Retinal waves were recently shown to travel in a preferred direction (Stafford et al., 2009); therefore, the correlation structure and directionality of waves carry information about retinal position, which is thought to instruct retinotopic map refinement, particularly along the nasal-to-temporal visual axis (Grubb et al., 2003; Cang et al., 2005; Chandrasekaran et al., 2005; Stafford et al., 2009).

Eye-specific refinement is thought to depend on the fact that retinal waves initiate at random locations and are separated by relatively long quiescent periods. These characteristics make it unlikely that RGCs in visuotopically matched positions in the two eyes will fire simultaneously. Based on these features of wave structure and on the fact that individual

inputs are initially weak during early postnatal development (suggesting multiple inputs may be required to bring a postsynaptic cell to threshold for an action potential (Liu and Chen, 2007)), prevailing instructive models for eye-specific refinement involve Hebbian plasticity mechanisms (Butts et al., 2007). The following paragraphs will briefly outline what we have learned from different activity manipulations regarding the viability of instructive Hebbian models.

In order to determine if specific spatiotemporal features of RGC activity instruct eye-specific segregation, one would like to alter the pattern of retinal activity without affecting overall activity levels. Unfortunately, such a manipulation has proved difficult to achieve. The first (and only) study that claimed to meet these criteria used an immunotoxin to kill starburst amacrine cells, the interneurons responsible for generating cholinergic waves, in ferret retinas (Huberman et al., 2003). The researchers found that 80% of starburst cells were depleted by immunotoxin treatment, which disrupted correlated firing between pairs of RGCs but did not alter the average firing rate of RGCs as a population. Eye-specific domains formed normally in the toxin-treated animals; consequently, the researchers concluded that retinal activity levels play a permissive role in eye-specific segregation. Their results were difficult to interpret, however, since some wave-like activity was observed in the treated retinas by calcium imaging, which raised the possibility that the components of waves that are required for segregation might have been intact in the toxin treated retinas. Another issue with the authors' interpretation was that even though the average firing rate of a population of RGCs was preserved after immunotoxin treatment, average activity levels in individual RGCs were not preserved (some RGCs were completely silent while others fired continuously). In a permissive model individual RGCs would need to achieve a certain level of activity in order undergo normal growth and refinement, thus it remains difficult to assess what the immunotoxin findings tell us about the role of retinal activity during eye-specific refinement.

A commonly used pharmacologic strategy for disrupting cholinergic retinal waves is intraocular injection of the nicotinic receptor agonist epibatidine, which faithfully blocks eye-specific segregation (Huberman et al., 2002; Koch and Ullian, 2010; Penn et al., 1998;

Pfeiffenberger et al., 2005; Rebsam et al., 2009; Stellwagen and Shatz, 2002; Sun et al., 2008). What are the effects of epibatidine on retinal waves? Based on whole cell retinal recordings and calcium imaging experiments researchers initially concluded that epibatidine blocked all retinal spiking during segregation (Huberman et al., 2002; Penn et al., 1998). More recent experiments using MEA recordings, however, showed that epibatidine treatment only blocked spiking in about 50% of RGCs and that the remaining 50% exhibited continuous firing (Sun et al., 2008). In any case, epibatidine experiments have strongly suggested that retinal spiking plays an important role in eye-specific refinement, but they have not offered much insight into nature of that role.

An extensively studied genetic model for disrupting cholinergic retinal waves is the beta2 knockout mouse, which lacks the beta2 subunit of the nicotinic acetylcholine receptor (Bansal et al., 2000; Cang et al., 2008a,b; Grubb et al., 2003; Grubb and Thompson, 2004; Muir-Robinson et al., 2002; Rossi et al., 2001; Shah and Crair, 2008). Similar to epibatidine treatment, beta2 removal was initially shown to abolish retinal waves and to prevent eye-specific refinement (Bansal et al., 2000; McLaughlin et al., 2003; Muir-Robinson et al., 2002; Rossi et al., 2001). Its affects on eye-specific refinement remain undisputed; however, the beta2 knockouts were subsequently shown to exhibit retinal waves when MEA recordings were performed at 37°C, a more physiologic temperature (Sun et al., 2008). Retinal activity was actually increased in beta2 mice compared to controls and was significantly altered in several key ways, 1) correlation strengths between pairs of RGCs did not diminish as steeply as a function of the distance between them (indicating that relatively distant RGCs within a wavefront exhibited more correlated spiking in beta2 knockouts than in wildtypes), 2) waves were more frequent and propagated faster in the beta2 knockouts, and 3) beta2 knockouts exhibited increased bursting between waves. These results were confirmed in a study by Stafford et al. (2009) in which the authors applied a larger, denser MEA to the question. In the latter study the authors offered a model for how the alterations in beta2 knockout waves lead to altered retinotopy and eye-specific segregation. They suggested that retinotopic mapping

errors were the result of the increased correlations exhibited between more distantly located RGCs in beta2 KO retinas, which could cause both neighboring and more distant pairs of RGCs to be active coincidentally with postsynaptic spiking, thereby stabilizing excess inputs. While this model could explain retinotopic mapping errors in the mutants, what about their lack of eye-specific segregation? Regarding this question the authors suggested that dramatically reduced inter-wave intervals and increased spiking between waves probably prevented eye-specific segregation by increasing the amount of coincident spiking between inputs arising from different eyes. Although both wave structure and overall activity levels are clearly altered in beta2 knockouts, the findings from the beta2 mutants are indeed consistent with a Hebbian model for eye-specific refinement.

Some doubt is cast on this model, however, when one considers other experimental manipulations that increased retinal wave activity. For instance, binocular injections of cAMP or forskolin were shown to increase wave frequency but did not prevent eye-specific refinement (Stellwagen and Shatz, 2002). In addition, genetic removal of the gap junction component connexin36 increased spiking between waves, but it too had no apparent effect on eye-specific refinement (Torborg et al., 2005). These findings call into question the role of quiescent inter-wave intervals in eye-specific refinement. Differences in the severity of the activity disruptions between these different experimental manipulations could help to explain their discrepant findings. It is difficult, however, to directly compare the studies since they were not performed under identical recording conditions. In theory, a side-by-side analysis of major the experimental models outlined above using identical recording conditions could serve to clarify the differences between their activity perturbations and thereby narrow in on the key activity features that drive eye-specific refinement. However, this issue will not be fully resolved until we can record, and ideally control, retinal activity patterns in vivo.

As it stands, the fact that certain wave manipulations block eye-specific segregation while others do not strongly suggests that particular features of retinal activity are more important for eye-specific refinement than others. However, the exact nature of the key

features continues to be elusive. Furthermore, whether the key activity features instruct eye-specific refinement or whether they induce a separate, instructive mechanism remains debatable.

1.6 Synaptic mechanisms implicated in eye-specific segregation

To move the field forward it would be useful to identify the downstream mechanisms that read-out retinal activity and translate it into functional and structural changes to RGC synapses and axons. Have particular synaptic mechanisms been implicated in eye-specific refinement?

A prerequisite of Hebbian instructive models is that correlated RGC inputs are capable of eliciting action potentials in postsynaptic dLGN neurons. As mentioned earlier, dLGN neurons receive weak inputs from many RGCs residing in both eyes during eye-specific refinement (Chen and Regehr, 2000; Ziburkus and Guido, 2006), and the minimum synaptic current required to elicit postsynaptic firing is larger than currents typically evoked by individual RGC inputs (Liu and Chen, 2008). A study by Mooney et al. (1996) used a thalamic preparation with the eyes still attached to show that bursts of action potentials in RGC axons drive postsynaptic action potentials in dLGN neurons. AMPARs were required for synaptic input to drive postsynaptic spiking, whereas NMDA receptors (NMDARs) were dispensable. A more recent slice physiology study found just the opposite, that NMDAR activation was necessary for triggering postsynaptic spikes, whereas AMPARs contributed to fidelity in the timing of the spikes (Liu and Chen, 2008). Is glutamatergic transmission required for eye-specific refinement? A study by Smetters et al., (1994) suggested that NMDAR activation might be dispensable. They delivered the NMDAR antagonist CPP systemically during the period of eye-specific segregation and found that NMDAR-blockade did not prevent eye-specific segregation; although NMDAR antagonists did prevent ON/OFF segregation in another study (Hahm et al., 1991). A glaring caveat of the experiment, however, was the lack of evidence demonstrating that NMDARs were effectively blocked at RGC-dLGN synapses during segregation. It is not known whether AMPAR activation or glutamate release from RGC axons is required eye-specific

refinement. Chapters 2 and 3 investigate the roles of synaptic glutamate release and AMPAR-mediate synaptic transmission, respectively, during eye-specific refinement.

Do RGC-dLGN synapses exhibit Hebbian synaptic plasticity? A 1993 study by Mooney et al. was the first to report an LTP-like plasticity mechanism in the dLGN; however, the plasticity-inducing protocol in that study used a higher stimulus frequency than is normally observed during retinal waves (100Hz) and only produced changes in synaptic strength in a small fraction of recorded dLGN neurons. In addition, it relied on NMDAR activation, which may not be required for eye-specific refinement; thus, the relevance of those findings is unclear.

A 2000 study from the Shatz laboratory (Huh et al., 2000) tried to link synaptic plasticity to eye-specific refinement by showing that mutants lacking in key components of the class 1 MHC pathway failed to undergo eye-specific segregation and showed enhanced LTP and no LTD at CA1 hippocampal synapses, thus suggesting that the unrefined ipsilateral projections exhibited by MHC pathway mutants might be due to failures in the synaptic plasticity mechanisms that underlie synapse elimination. A major caveat of the study was that the researchers did not report any physiological deficits at RGC-dLGN synapses, and MHC 1 function may vary across brain regions (Huh et al., 2000; Letellier et al., 2008). In addition, a subsequent study showed that eye-specific refinement occurs and is normal in MHC pathway mutants at P10 (Xu et al., 2010). Eye-specific projections then desegregated after P10. The study then showed that retinal waves were highly abnormal in the mutants during the period when their ipsi and contra axons desegregated. Therefore, it is difficult to discern whether the MHC pathway contributes to eye-specific axon refinement through synaptic mechanisms in the dLGN or through the regulation of retinal waves or both.

Butts et al. were the first to demonstrate Hebbian synaptic plasticity in the dLGN (2007). They showed that when 10Hz optic tract bursts (a frequency commonly observed during normal retinal waves) were paired with postsynaptic spikes, synaptic strengthening could be elicited (~20% increase in EPSC size), and when presynaptic bursts were separated

from the postsynaptic spike by 1 second intervals, mild synaptic depression occured (~10% decrease in EPSC size). The plasticity mechanism, which the authors termed "burst-timing dependent", is consistent with an instructive Hebbian model. While the magnitude of the plasticity was quite small, its cumulative effects over weeks could be more substantial. The timing window reported for the plasticity may differ during normal retinal waves, however, since dLGN neurons typically fire bursts of action potentials in response to retinal input, as opposed to the single spikes presented in the plasticity inducing protocol (Mooney et al., 1996). In addition, while it is easy to see how this form of plasticity could contribute to the refinement of inputs within an eye, it is less clear how it would distinguish inputs from the two eyes. For instance, dLGN neurons are initially innervated by a group of RGCs in the left eye and a group of RGCs in the right eye. When a wave occurs in the left eye some of the left-eye inputs will fire synchronously and elicit postsynaptic spiking, while other inputs (those that are on the far end of the wave domain or outside the wave domain) would not be well synchronized with the postsynaptic activity. The synchronous inputs would be strengthened and the others would undergo depression, thus left-eye retinotopy would be sharpened. The same would also be true for the right-eye inputs. Consequently, this form of plasticity would strengthen synchronously-firing inputs in the left eye and synchronously-firing inputs in right eye; thereby preventing eye-specific segregation. Whether Hebbian plasticity mechanisms are capable of driving eye-specific refinement may depend on the exact spatial distribution of the RGCs in the two eyes that innervate individual dLGN neurons. Unfortunately, it is not presently possible to back-label the RGCs that innervate single dLGN neurons.

A third type of plasticity was reported by Ziburkus et al. (2009). These authors found that when they stimulated groups of RGC axons with parameters that mimicked retinal waves (though stimulus frequencies were on the high end of what has been reported for retinal waves) the stimulation triggered long-term depression in dLGN neurons that was NMDAR and GABAR independent and required L-type calcium channel activation. Later in development, after eye-specific territories formed, the same stimulus protocol elicited mild synaptic

potentiation. The authors did not monitor or manipulate postsynaptic spiking. That form of plasticity is quite different from the plasticity reported by Butts et al. since the synchronous activation of many RGC inputs led to synaptic depression, where as Hebbian plasticity would strengthen coincident inputs. It's unclear how this plasticity mechanism alone could distinguish appropriate inputs from inappropriate inputs. Regardless, it could certainly contribute to synaptic weakening during eye-specific refinement, and the authors made the argument that synaptic depression may be the major form of plasticity during eye-specific refinement since the major phase of input strengthening occurs after P10.

Importantly, it is not currently known if any of the plasticity mechanisms outlined above are present at RGC-dLGN synapses in vivo of if they participate in eye-specific refinement. Furthermore, while retinal activity is required for axonal refinement, no studies have demonstrated a requirement for synaptic transmission per se. Better methods for directly manipulating RGC-dLGN synapses in vivo are clearly needed to shed light on the precise roles played by synaptic transmission and plasticity in refining eye-specific circuit connections.

1.7 What lies ahead

In chapter 2 a novel mouse genetic strategy was employed to directly manipulate glutamate release from RGC axons in vivo. The strategy allowed us to reduce synaptic glutamate release specifically from ipsilateral-projecting RGC axons; thereby introducing a bias into the competitive interactions between contralateral and ipsilateral synapses —a bias against the poorly transmitting ipsilateral-RGC axons. Thus, pathway-specific attenuation of glutamate release allowed for the investigation of the direct roles played by glutamate-based synaptic competition in eye-specific visual circuit refinement.

Chapter 3 focuses on the roles of two proteins, neuronal pentraxins 1 and 2 (NP1/2), during retinogeniculate development. Previous studies showed that eye-specific segregation was disrupted in mice lacking NP1/2. In addition, several cell culture studies have suggested that NP1/2 play important roles in the development of AMPAR-mediated glutamatergic synaptic

transmission. Based on these findings we viewed NP1/2 as potential participants in the activity-dependent refinement of RGC axons and synapses. The experiments in chapter 3 investigated the requirement for NP1/2 in the normal development of AMPAR-mediated transmission at RGC-dLGN synapses, and they began to explore the relationship between the physiological and anatomical defects displayed by NP1/2 knockout mice.

Finally, the discussion section attempts to relate the two studies, and it suggests future experiments which could extend the present studies and thereby get us closer to defining the synaptic mechanisms that drive axonal refinement within developing CNS circuits.

Chapter 2

Pathway-specific genetic attenuation of glutamate release alters select features of competition-based visual circuit refinement

This chapter investigates the role of glutamate-based synaptic competition in the eye-specific patterning of RGC-dLGN connections. It contains a modified version of our manuscript that is in press at the journal Neuron.

2.1 Results

2.1.1 A genetic approach to selectively alter gene expression in ipsilateral-projecting RGCs

To investigate the role of synaptic transmission in visual circuit refinement we aimed to selectively disrupt synaptic glutamate release in one population of competing RGC axons. The serotonin transporter is known to be highly restricted to the ipsilateral-projecting population of RGCs during development (Garcia-Frigola and Herrera, 2010; Narboux-Neme et al., 2008; Upton et al., 1999). We therefore screened several SERT-Cre lines to determine whether any of them expressed Cre specifically in ipsilateral RGCs (Gong et al., 2007). In addition, because dLGN neurons also express the serotonin transporter during development (Lebrand et al., 1996; Narboux-Neme et al., 2008), we sought Cre lines with no SERT-Cre expression in dLGN neurons. One founder line, ET33 SERT-Cre (see experimental methods for details on obtaining these mice), was a promising candidate for meeting these criteria; consequently, we crossed the ET33 SERT-Cre to various reporter mice to determine the spatial and temporal pattern of Cre expression in ET33 SERT-Cre mice.

Previous studies have shown that ipsilateral-projecting RGCs in mice reside in a crescent shaped portion of the peripheral ventral-temporal retina (Drager and Olsen, 1980; Dreher et al., 1985; Farid Ahmed et al., 1998; Herrera et al., 2003) (Figure 2.1A); we therefore examined the location of the Cre-expressing RGCs in whole-mounted and sectioned retinas by crossing the ET33-Cre mouse to various floxed reporter mice to label Cre-expressing cells

(Figure 2.1B,C,D). Indeed, when crossed to LacZ (Soriano, 1999), membrane targeted GFP (Hippenmeyer et al., 2005) or tdTomato (Ai9; Madisen et al., 2009) reporter mice, we found that the spatial distribution of the Cre-expressing cells matched the predicted distribution for ipsilateral RGCs (Figure 2.1B,D), with an additional thin strip of cre-expression observed in the dorsal-nasal retina (Figure 2.1B). A highly similar pattern of expression has been reported for SERT (Garcia-Frigola and Hererra, 2009). The vast majority of Cre-expressing cells were RGCs since they were located predominantly in the RGC layer of the retina (Figure 2.1D) and they extended axons to the optic nerve head (Figure 2.1C).

Next we examined the pattern of retinogeniculate projections labeled by Cre-driven expression of fluorescent protein (mGFP or tdTomato), and compared that pattern to the pattern of RGC axonal projections labeled by fluorescently conjugated cholera toxin beta. Figure 1E shows the pattern of retinogeniculate reporter expression one would predict in a Cre line that faithfully labels the ipsilateral RGC population. The genetically labeled axons should overlap exclusively with the CTb-labeled axons that project ipsilateral to the injected eye (Figure 2.1F). Indeed, we found a direct correspondence between the genetically labeled Cre-expressing RGC axons (Figure 2.1I, ice blue) and the CTb-labeled ipsilateral RGC axons (Figure 2.1H, magenta) (Figure 2.1J, white indicates overlap). In addition, as is typical for a P12 mouse, we found very little overlap between the CTb-labeled contralateral (Figure 2.1G, green) and ipsilateral axons (overlap shown in Figure 2.1K). The image of the CTb-labeled RGC projections from the contralateral and ipsilateral eyes, merged with the image of the Cre-driven genetically labeled axons readily shows that the genetically labeled axons overlapped with the ipsilateral axons and did not correspond with axons arising from the contralateral eye (Figure 2.1L). In addition, we noted that a small population of Cre reporter-labeled axons was also present in the intergeniculate leaflet (a relatively thin nucleus that resides between the dLGN and vLGN). Finally, to be certain that the genetically labeled axons in the dLGN arose exclusively from the ipsilateral eye, we removed one eye from a ET33-Cre::tdTomato mouse and retinogeniculate projections were visualized two weeks later, allowing sufficient time for

the RGC axons from the enucleated eye to degenerate. Axons from the remaining intact eye displayed a robust projection to the dLGN on the same side of the brain, whereas the dLGN on the opposite (contralateral) side of the brain was devoid of signal (Figure 2.2A,B). Moreover, little to no Cre expression was apparent in dLGN neurons in ET33-Cre mice (Figure 1I) (Figure 2.2B). This experiment also revealed that the small projection from Cre-expressing RGCs to the intergeniculate leaflet is purely contralateral (Figure 2.2B) which may account for the small cohort of Cre RGCs in the dorso-nasal retina (Figure 2.1B). Collectively, these data indicate that in ET33-Cre mice, Cre is expressed by the RGCs that project to the ipsilateral but not the contralateral dLGN.

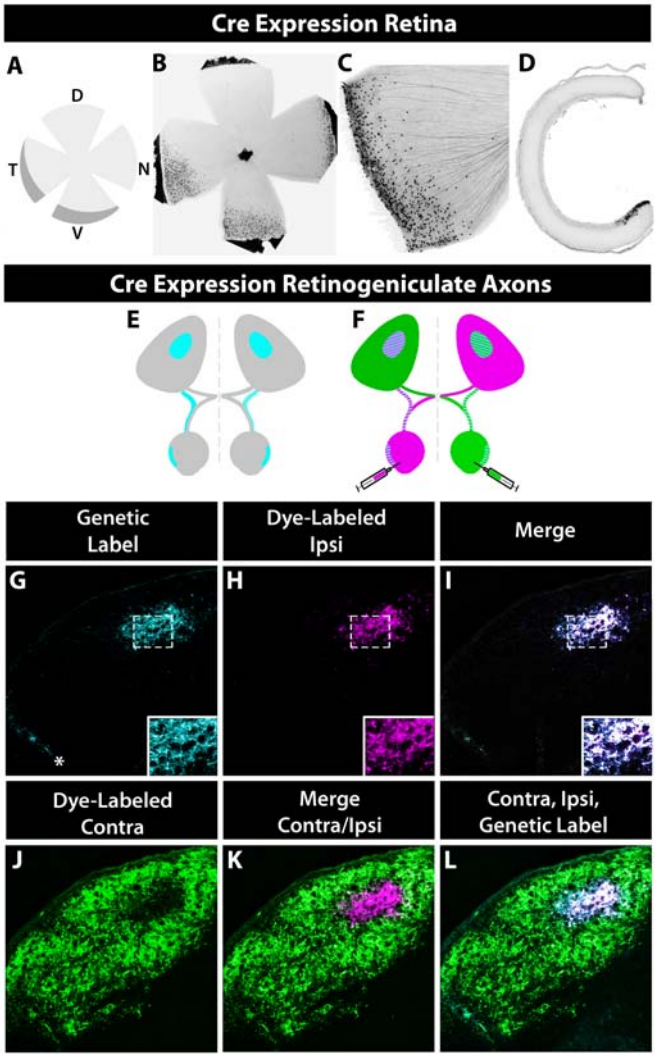

Figure 2.1 Transgenic mouse that expresses Cre selectively in ipsilateral-projecting RGCs. (A) Diagram of flat mounted retina showing the location of ipsi-RGCs (Herrera et al., 2003). (B) Xgal stained ET33-Cre retina. (C) tdTomato expression shows RGC axons coursing toward the optic nerve head. (D) Retinal cross section shows reporter in the RGC layer (P0). (E) Diagram shows expression in RGC-dLGN pathway of an ipsi-specific Cre animal. (F) Diagram compares reporter expression to dye-labeled afferents. (G) Reporter expression in the dLGN of a P12 ET33 animal (ice blue). Asterisk indicates IGL. (H) Dye-labeled ipsilateral axons (magenta). (I) Merger of genetically-labeled and dye-labeled ipsi axons (Overlap in white). (J) Dye-labeled contra axons (green). (K) Overlay dye-labeled ipsi and contra axons. (L) Genetically-labeled axons and dye-labeled axons merged.

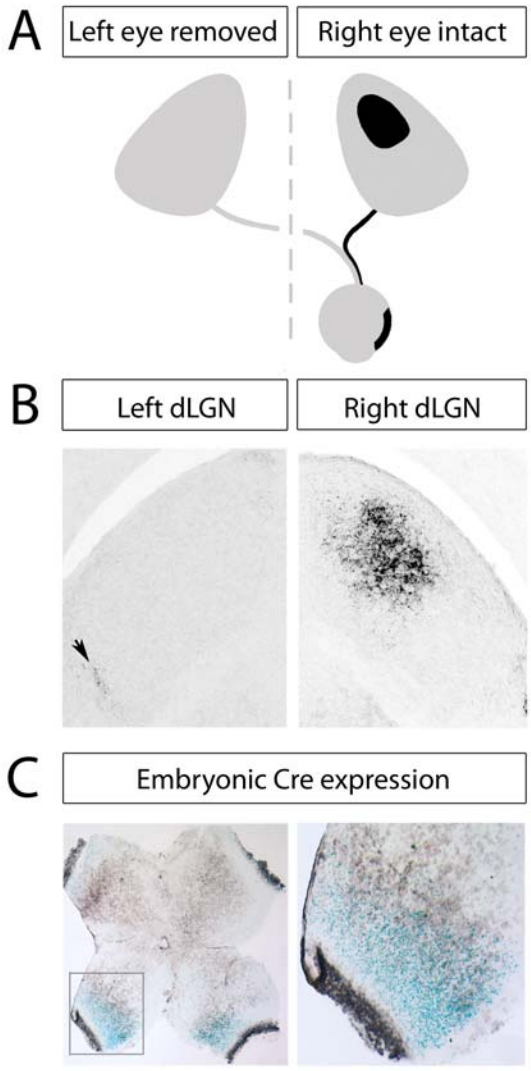

Figure 2.2 Cre-driven reporter expression in ET33 Sert-Cre mice is restricted to ipsilateral-projecting RGCs and initiates embryonically.

(A) Diagram of an experiment in which one eye (left) was removed and its axons allowed to degenerate, thereby allowing the visualization of the axonal projections arising from a single eye (right). (B) The remaining eye sends reporter-labeled axons to the dLGN on the same side of the brain (right image), but not to the dLGN on the opposite side of the brain (left image). Arrow in the left image points to a small crossed projection of reporter-expressing axons outside of the dLGN, in the intergeniculate leaflet. (C) Xgal staining reveals robust Cre-driven reporter expression in an embryonic retina at E18.

2.1.2 Pathway specific attenuation of vesicular glutamate release

The finding that Cre is expressed specifically by ipsilateral projecting RGCs in ET33-Cre mice offered the powerful opportunity to selectively alter gene expression in that cohort of RGCs in vivo. Our goal was to disrupt glutamatergic synaptic transmission arising from ipsilateral RGCs during the period of eye-specific circuit refinement. Vesicular glutamate transporter 2 (VGlut2) is the only vesicular glutamate transporter expressed by RGCs (Fujiyama et al., 2003; Hayakawa and Kawasaki, 2010; Johnson et al., 2003; Sherry et al., 2003; Stella et al., 2008) and VGlut2 is required for synaptic glutamate release (Hnasko et al., 2010; Stuber et

al., 2010). Thus, we mated ET33-Cre mice to mice that carry floxed alleles of the vesicular glutamate transporter 2 (VGlut2) (Hnasko et al., 2010) and thereby generated ET33-Cre::VGlut2$^{flox/flox}$ offspring which lack VGlut2 specifically in ipsilateral-projecting RGCs. In the mouse expression of VGlut2 protein is low in the late embryonic period, becomes detectable at P0 and increases dramatically over the first postnatal week of life (Sherry et al., 2003; Stella et al., 2008). Importantly, we found that Cre expression in ET33-Cre mice initiates embryonically, at least as early as embryonic day 18 (Figure 2.2C). When we cultured RGCs from P3 ET33-Cre mice expressing either wild-type or floxed VGlut2 and immunostained them on P5 we found that VGlut2 immunofluorescence intensity was dramatically and significantly reduced specifically within the ET33-Cre::VGlut2$^{flox/flox}$ RGCs (Figure 2.3A-G). Eye-specific segregation in the mouse dLGN occurs largely between P4-P10. Thus, the expectation was that ET33-Cre::VGlut2$^{flox/flox}$ mice should exhibit reduced glutamate release from their ipsilateral RGCs during and after the period of eye-specific segregation.

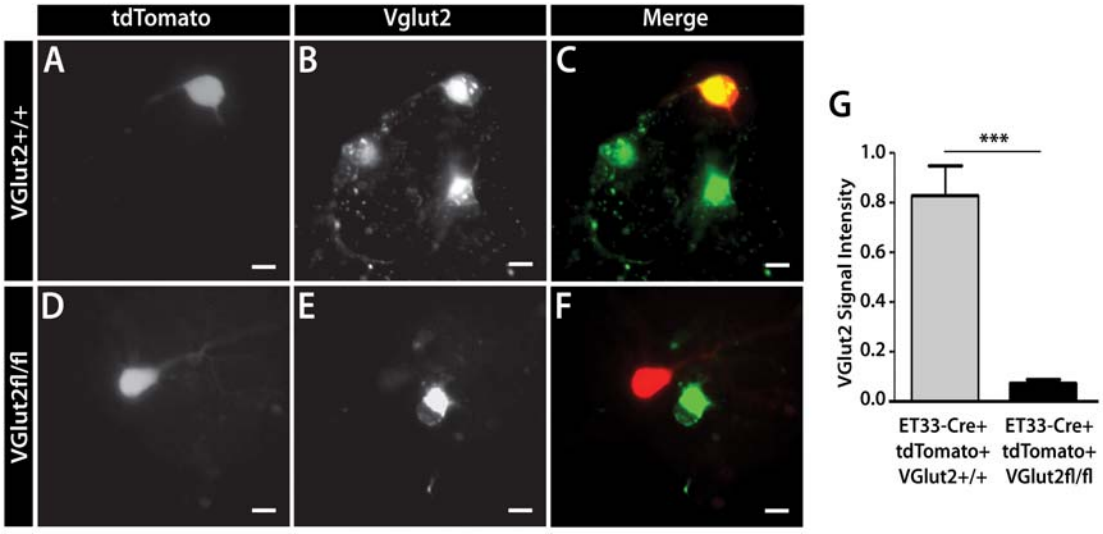

Figure 2.3 Loss of VGluT2 immunoreactivity in ET33-Cre::VGluT2$^{flox/flox}$ RGCs. (A-G) Retinal cells were dissociated from P3 mice expressing ET33-Cre, floxed-stop-tdTomato, and either VGlut2$^{+/+}$ or VGlut$^{flox/flox}$. Immunostaining performed on DIV2. (A-F) Example images showing tdTomato positive cells (A,D), VGlut2 immunofluorescence (B,E), and merged images. Scale bar=10µm. (G) Average VGlut2 signal intensity, normalized to soma size (n=20 VGlut2$^{+/+}$ cells and n=16 VGlut2$^{flox/flox}$ cells; p<0.0005).

To test whether retinogeniculate transmission is indeed altered in ET33-Cre::VGlut2$^{flox/flox}$ mice, we recorded electrophysiological responses of dLGN neurons in response to optic tract stimulation from ET33-Cre::VGlut2$^{flox/flox}$ mice and littermate control VGlut2$^{flox/flox}$ mice lacking Cre. We prepared brain slices containing the optic tract and dLGN, which allowed us to simultaneously stimulate the optic tract and record postsynaptic responses in whole-cell voltage-clamped dLGN neurons (Chen and Regehr, 2000: Koch and Ullian, 2010). Because the optic tract contains axons from both eyes it was necessary to first remove one of the two eyes in vivo and then allow a period of time for the axons from the enucleated eye to degenerate before preparing slices and recording from the dLGN contralateral or ipsilateral to the intact eye (see Figure 2.4A,B for images of slices). In addition, we injected CTb into the intact eye in order to visualize its axonal projections within the dLGN slice preparation and to target the recording electrode to the appropriate ipsi-eye or contra-eye innervated portion of the dLGN (Figure 2.4B). In one set of experiments, we enucleated mice on P0 and recorded from them on P5, an age when the RGC axons from the two eyes are still largely overlapping in the dLGN (Jaubert-Miazza et al., 2005). In another set of experiments we enucleated mice on P5 and recorded from them on P10.

In P5 slices stimulation of contralateral RGC axons faithfully produced postsynaptic NMDAR-mediated responses in every dLGN neuron tested regardless of genotype, and the size of the contralateral NMDAR-mediated responses were indistinguishable between Cre-expressing and Cre-negative slices (Figure 2.4C,E; VGlut2$^{flox/flox}$ = 1006+/-138.69pA, n=11 and ET33-Cre::VGlut2$^{flox/flox}$ = 1102+/-176.1pA, n=11; $p>0.05$). By contrast, when ipsilateral RGC axons were stimulated postsynaptic responses were faithfully produced only in Cre-negative VGlut2$^{flox/flox}$ slices, whereas in ET33-Cre::VGlut2$^{flox/flox}$ slices postsynaptic currents were observed in just half of the dLGN neurons tested (13 out of 24) and response sizes were reduced to ~45% of controls (Figure 2.4D,F; VGlut2$^{flox/flox}$ mice = 343.75+/-59.21 pA, n=19 and ET33-Cre::VGlut2$^{flox/flox}$ mice = 157.49+/-40.51pA, n=22; $p=0.014$ by Mann-Whitney). Analysis of

the AMPAR-mediated component of the postsynaptic responses yielded similar results (Figure 2.5).

To determine the state of synaptic transmission in ET33-Cre::VGlut2$^{flox/flox}$ mice during later stages of retinogeniculate refinement we recorded dLGN responses on P10, an age when ongoing spontaneous activity continues to refine and maintain eye-specific retinogeniculate projections (Chapman, 2000; Demas et al., 2006; reviewed in Huberman et al., 2008a). We found that, similar to P5, P10 contra responses remained at control levels in ET33::VGlut2$^{flox/flox}$ slices (Figure 2.4E,G; VGlut2$^{flox/flox}$ = 1136+/-126.26pA, n=14 and ET33-Cre::VGlut2$^{flox/flox}$ = 1136.36+/-126.19pA, n=12; $p>0.05$) and P10 ipsilateral responses continued to be reduced in ET33::VGlut2$^{flox/flox}$ slices compared to controls (Figure 2.4F,H; VGlut2$^{flox/flox}$ = 256.08+/-49.90pA, n=17 and ET33-Cre::VGlut2$^{flox/flox}$ = 7.54+/- 3.60pA, n=22; $p<0.0001$ by Mann-Whitney). The deficit in ipsilateral synaptic transmission exhibited by P10 ET33-Cre::VGlut2$^{flox/flox}$ mice was more pronounced than the deficit observed on P5. In P10 ET33-Cre::VGlut2flox/flox slices only 18% of dLGN neurons responded to ipsi axon stimulation (4 of 22 compared to 17 of 19 or 89% in controls) and their average response amplitudes were reduced to just ~3% of control responses. AMPAR-mediated ipsilateral responses in ET33-Cre::VGlut2$^{flox/flox}$ slices were also further diminished between P5 and P10 (Figure 2.5). Collectively, our electrophysiological findings demonstrate that glutamatergic synaptic transmission is selectively and progressively lost from the ipsilateral retinogeniculate pathway in ET33-Cre::VGlut2$^{flox/flox}$ mice.

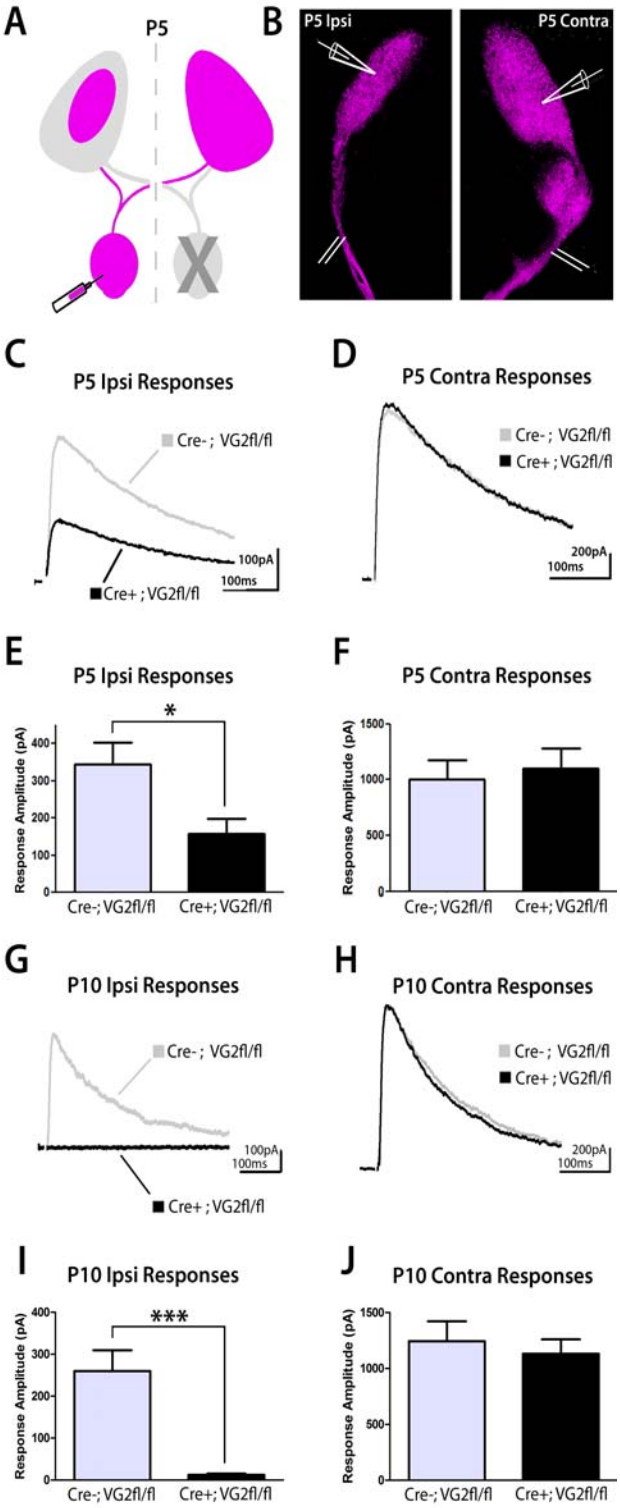

Figure 2.4 ET33-Cre driven knockout of VGlut2 reduces NMDAR-mediated synaptic currents in the ipsilateral RGC-dLGN pathway. (A) Diagram shows removal of one eye and remaining projections. (B) Slices containing ipsi (left) and contra (right) projections and showing positions of stimulating and recording electrodes. (C) Example traces from P5 littermates showing postsynaptic NMDAR-mediated responses recorded in response to selective stimulation of ipsilateral axons. (D) Responses to contralateral axon stimulation at P5. (E) Average response amplitudes (in pA) from ipsilateral axon stimulation at P5 (VGlut2$^{flox/flox}$ mice = 343.75+/-59.21 pA, n=19 and ET33-Cre::VGlut2$^{flox/flox}$ mice = 157.49+/-40.51pA, n=22; p=0.014 by Mann-Whitney). (F) Average response amplitudes of contralateral responses at P5 (VGlut2$^{flox/flox}$ = 1006+/-138.69pA, n=11 and ET33-Cre::VGlut2$^{flox/flox}$ = 1102+/-176.1pA, n=11; p>0.05). (G) Examples of responses to ipsi-axon stimulation at P10. (H) Responses to contra-axon stimulation at P10. Note the near complete absence of transmission at this age. (I) Quantification of ipsi responses at P10 (VGlut2$^{flox/flox}$ = 256.08+/- 49.90pA, n=17 and ET33-Cre::VGlut2$^{flox/flox}$ = 7.54+/- 3.60pA, n=22; p<0.0001 by Mann-Whitney). (J) Average contra responses at P10 (VGlut2$^{flox/flox}$ = 1136+/-126.26pA, n=14 and ET33-Cre::VGlut2$^{flox/flox}$ = 1136.36+/-126.19pA, n=12; p>0.05).

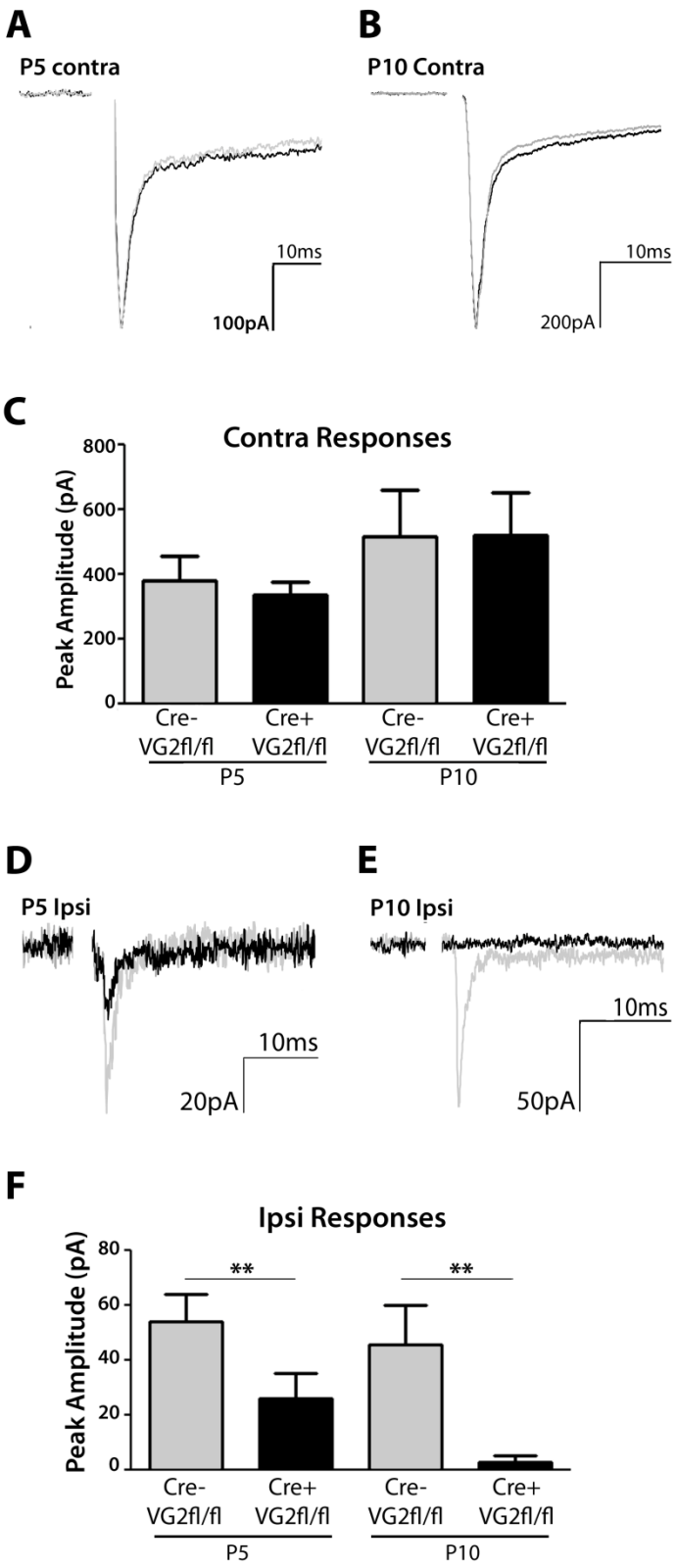

Figure 2.5 ET33-Cre driven VGlut2 removal reduces AMPAR-mediated synaptic currents in the ipsilateral RGC-dLGN pathway. (A) Examples of P5 contra responses. (B) Examples of P10 contra responses. (C) Ave contra responses (bars inverted). At P5 control contra responses were -381.5+/-76.48pA (n=11) and ET33-Cre::VGlut2$^{flox/flox}$ responses were -335.2+/-40.15pA (n=11; p>0.05 by a Student's T-test). At P10 control responses were -516.7+/-142.10 pA (n=6) and ET33-Cre::VGlut2$^{flox/flox}$ responses were -520.7+/-131.69pA (n=6; p>0.05 by a Student's T-test). (D) Examples of P5 ipsi responses. (E) Examples of P10 ipsi responses. (F) Average ipsi responses (bars inverted). At P5 average ipsi responses were -54.26+/-9.69pA for VGlut2$^{flox/flox}$ (n=19) and -26.11+/-9.14pA for ET33-Cre::VGlut2$^{flox/flox}$ (n=24; p<0.01 by Mann-Whitney). At P10 ipsi responses were -45.75+/-14.51 pA for VGlut2$^{flox/flox}$ (n=12) and -3.01+/-7.71pA for ET33-Cre::VGlut2$^{flox/flox}$ (n=13; p<0.01 by a Student's T-test).

2.1.3 Attenuation of glutamatergic transmission impacts select aspects of retinogeniculate refinement

What role does synaptic competition play in eye-specific retinogeniculate refinement? To address this question we analyzed the pattern of ipsilateral and contralateral RGC projections to the dLGN at different developmental stages in ET33-Cre::VGlut2$^{flox/flox}$ animals by labeling axons from the two eyes with CTb-488 or CTb-594 .

In WT P4 mice contralateral axons extend over the entire dLGN and ipsilateral axons are diffuse and spread out over a relatively large area of the target. Consequently, ipsilateral and contralateral axons show a high degree of overlap at this age (Godement et al., 1984; Jaubert-Miazza et al., 2005; Muir-Robinson et al., 2002; Pfeiffenberger et al., 2005). We found that both Cre negative and Cre expressing VGlut2$^{flox/flox}$ littermates exhibited axonal projection patterns typical for WT P4 mice (Figure 2.6A-C). Thus, prior to the period of eye-specific refinement the targeting of RGC axons is normal in ET33::VGlut2$^{flox/flox}$ animals.

Next we assessed the effect of altering relative synaptic activity levels on axonal refinement by imaging the pattern of RGC-dLGN projections at P10, an age when eye-specific segregation is normally largely completed (Jaubert-Miazza et al., 2005; Muir-Robinson et al., 2002) (Figure 2.6A). Based on existing models and studies of eye-specific refinement (and previous results of altering RGC activity levels in one eye (Butts et al., 2007; Koch and Ullian, 2010; Penn et al., 1998; Stellwagen and Shatz, 2002; reviewed in Huberman et al., 2008a), one would predict that impairing vesicular glutamate release in ipsilateral axons would place them at a severe competitive disadvantage compared to fully active contralateral eye axons, and would lead to i) a failure of contralateral eye axons to retract from ipsi-eye territory, and ii) a corresponding dramatic reduction in ipsilateral eye territory in the dLGN.

Indeed, we found that in the ET33::VGlut2$^{flox/flox}$ mice, contralateral eye axons from the failed to retract from the ipsilateral region of the dLGN (Figure 2.6A); the ET33-Cre::VGlut2$^{flox/flox}$ mice contained contralateral RGC axons throughout their entire dLGN (Figure

2.6A) and thus, a significantly greater degree of overlap between ipsilateral and contralateral axons compared to controls of the same age (Figure 2.6D; n=8 mice for each genotype). The increased overlap observed in the VGlut2 knockouts was statistically significant over a wide range of signal-to-noise threshold values (p values displayed in Figure 2.6D and associated figure legend) (thresholding procedure is described in the methods section as was performed as in Bjartmar et al., 2006; Rebsam et al., 2010; Torborg et al., 2005). These data provide genetic evidence that synaptic transmission based mechanisms underlie axon-axon competition between pathways from the two eyes during neural circuit refinement.

The results of reducing synaptic transmission in ipsilateral eye axons were, however, surprising when we analyzed the overall pattern of the ipsilateral retino-dLGN terminal field. As noted above, a consistent observation in pharmacologic studies of eye-specific refinement is that drugs that disrupt or increase retinal activity in one eye cause the axons arising from the less active eye to lose territory in the dLGN (Koch and Ullian, 2010; Penn et al., 1998; Stellwagen and shatz, 2002; reviewed in Huberman et al., 2008a). Despite the clear lack of eye-specific refinement in ET33-Cre::VGlut2$^{flox/flox}$ animals at P10, the territory occupied by the glutamate release deficient axons appeared normal in shape and size (Figure 2.6A,E). That is, despite being completely intermingled with contralateral eye axons, all ET33-Cre::VGlut2$^{flox/flox}$ animals displayed ipsilateral projections that overall, were indistinguishable from that of control animals (Figure 3E). Ipsi-eye axons extended over 10.68+/-0.44% of the dLGN in VGlut2$^{flox/flox}$ animals and over 13.03+/-1.63% in ET-33-Cre::VGlut2$^{flox/flox}$ animals (n=8 mice for each genotype, $p>0.05$). Thus, despite having markedly reduced glutamate release throughout the major phase of eye-specific segregation from P5-P10 (Figures 2.4 and 2.5), the genetically altered ipsi-eye axons maintain the ability to consolidate their normal amount of dLGN territory (Figure 2.6A,D; Figure 2.7).

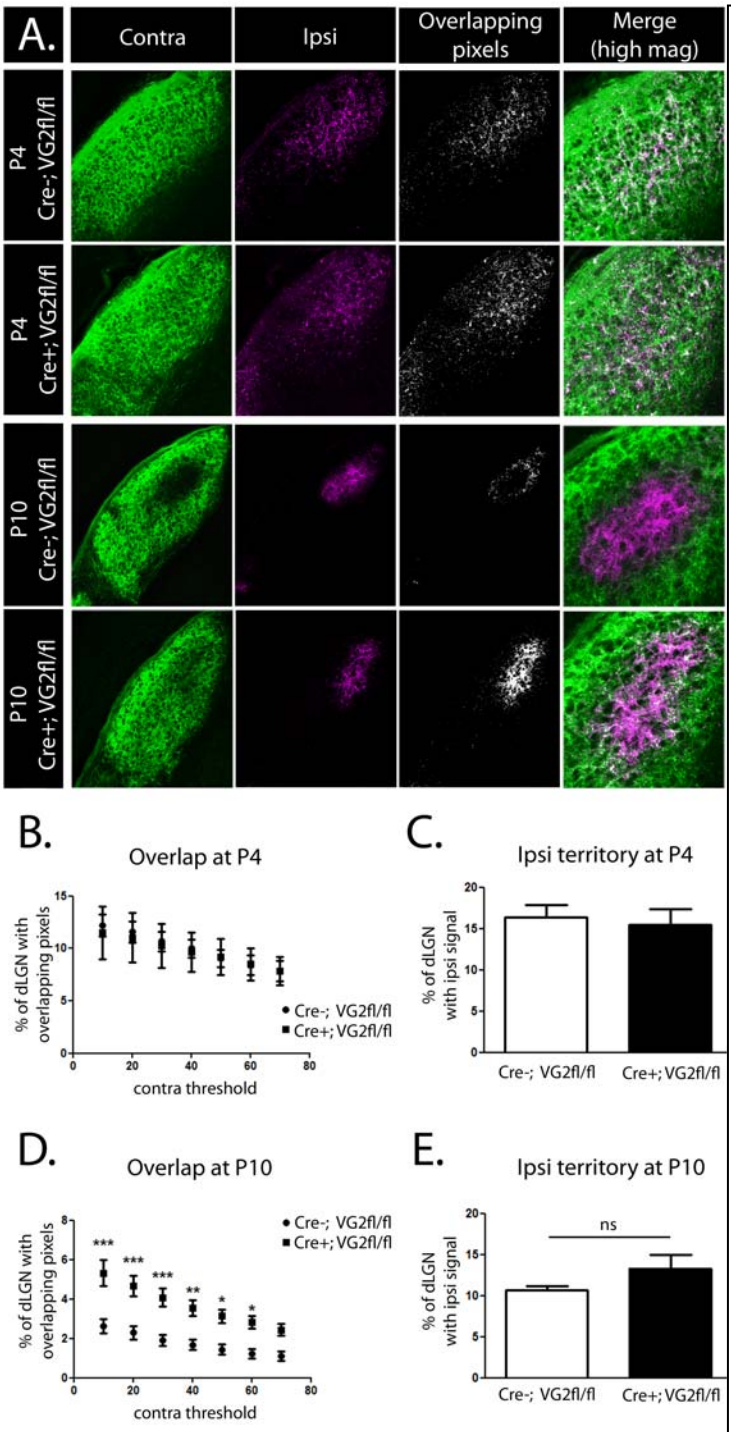

Figure 2.6 Reduced ipsi-RGC synaptic transmission perturbs eye-specific refinement but not the consolidation of ipsi-eye territory in the dLGN. (A) Dye-labeled RGC axons in Cre- and Cre+ VGlut2$^{flox/flox}$ animals at P4 (upper two rows) and P10 (lower two rows). First column shows contra-RGC axons (green), second column ipsi-RGC axons (magenta), third column overlapping contra and ipsi axons (white), and fourth column shows a higher mag. image of the region of overlap (white). **(**B) Percent of dLGN pixels that with overlapping contra and ipsi signal at P4 (n=6 per genotype). Overlap quantified over a range of noise threshold values. Two-way ANOVA revealed no significant differences. (C) Amount of ipsi-eye territory as a percent of total dLGN area. (D) P10 overlap (***p<0.001, **p<0.01, *p<0.05 by two-way ANOVA, n=8 per genotype). (E) Amount of ipsi signal at P10 (ipsi-eye axons occupied 10.68+/-0.44% of dLGN in controls and 13.03+/-1.63% in ET-33-Cre::VGlut2$^{flox/flox}$ mice, per genotype, p>0.05).

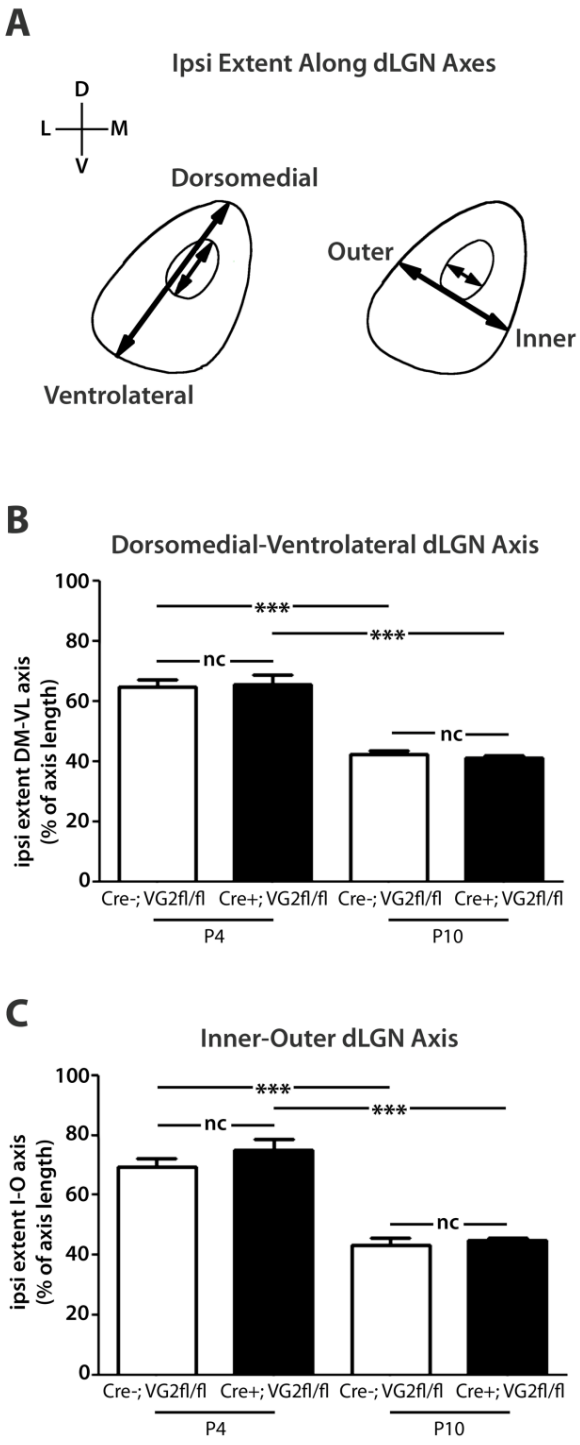

Figure 2.7 Ipsilateral RGC axons exhibit normal territory consolidation despite severely impaired synaptic glutamate release. (A) Diagram showing how the extent of the ipsilateral territory was measured over the two dLGN axes. (B) Length of the ipsilateral territory along the dorsomedial-to-ventrolateral dLGN axis at P4 and P10. In control animals ipsilateral axons extended over 64.67+/-2.34% (N=6) of the DM-to-VL axis at P4 and 42.11+/-1.23% at P10 (N=8); indicating a ~35% consolidation between the two ages ($p<0.001$ by Student's T-test). Similar results were obtained when VGluT2 was removed from the ipsilateral-projecting population. In ET33-Cre::VGluT2$^{flox/flox}$ mice ipsilateral axons extended over 65.36+/-3.24% of the DM-to-VL axis at P4 (N=6) and 41.07+/-0.77% at P10 (N=8) ($p<0.001$ by Student's T-test). No differences were found between VGluT2$^{flox/flox}$ and ET33-Cre::VGluT2$^{flox/flox}$ littermates at either age (at both ages $p>0.05$ by a Student's T-test). (C) Length of the ipsilateral territory along the inner-to-outer dLGN axis at P4 and P10. In control animals ipsilateral axons extended over 69.23+/-2.74% (N=6) of the DM-to-VL axis at P4 and 43.25+/-2.15% at P10 (N=8) ($p<0.001$ by Student's T-test). In ET33-Cre::VGluT2$^{flox/flox}$ mice ipsilateral axons extended over 74.75+/-3.47% of the DM-to-VL axis at P4 (N=6) and 44.73+/-0.73% at P10 (N=8) ($p<0.001$ by Student's T-test). The genotypes were not different at either age ($p>0.05$ at both ages by Student's T-test).

We next asked whether the consolidation of the diffuse ipsi-RGC axons observed on P4 into the more focal ipsi patch observed on P10 in ET33-Cre::VGluT2$^{flox/flox}$ animals (Figures 2.6 and 2.7) was driven by the presence of the glutamate-releasing contralateral axons. Contra-eye axons were removed from the dLGN by enucleating one eye in P1 pups. Ipsi-RGC axons from the remaining eye were imaged on P9/10. Similar to WT ipsi-RGC axons, the VGluT2-deficient ipsi-RGC axons formed a dense projection over a much larger portion of the dLGN at P9/10 when their glutamate-releasing competitors were absent Figure 2.8). This finding indicates that, even though glutamate-releasing contra-eye axons were unable to eliminate ipsi-eye axons from the dLGN, the contra-eye axons were responsible for restricting VGluT2-deficient ipsi-eye axons to their normal eye-specific region.

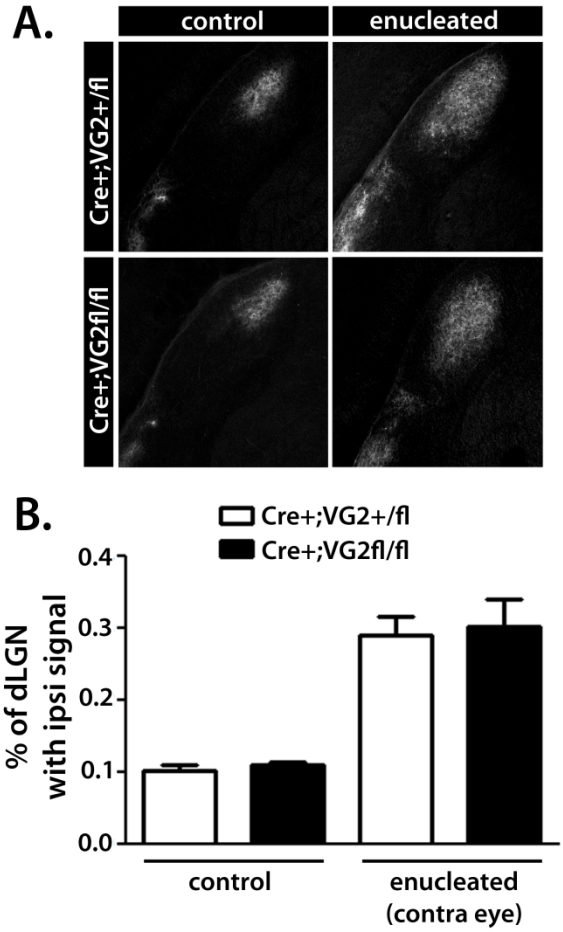

Figure 2.8 Expansion of VGluT2-deficient ipsi-RGC axons in the absence of contra-RGC axons.

(A) Examples of ipsilateral projections in Cre+;VG2+/fl (top row) and Cre+;VG2fl/fl animals (bottom row) under control conditions where both eyes were present (left column) and when the contralateral eye was removed (right column).

(B) Quantification the amount of ipsilateral signal under controls conditions and when competing.

Spontaneous retinal activity continues beyond P10 and is required to maintain eye-specific segregation during the subsequent developmental stage (Bansal et al., 2000; Chapman, 2000; Demas et al., 2006; reviewed in Huberman et al., 2008a). We therefore wondered if the loss of VGlut2 in ipsi-RGCs would eventually cause them to cede territory to the more active contra-eye axons. We examined RGC axonal projections in ET33-Cre::VGlut2$^{flox/flox}$ mice on postnatal day 28 (P28), which is ~2 weeks after eye-opening. Not surprisingly, P28 ET33-Cre::VGlut2$^{flox/flox}$ mice had contralateral RGC axons distributed throughout the entire dLGN (Figure 2.9A,B; n=7 mice per genotype, see figure and legend for p values), similar to what was observed in these mice on P10 (Figure 2.6A,D,E). However, despite having been at a competitive disadvantage to contra eye axons since at least P5, a period of about 3 weeks, the size of the ipsi-eye territory was not diminished in the P28 ET33-Cre::VGlut2$^{flox/flox}$ animals compared to control mice of the same age (Figure 2.9A,C). The ipsi-eye axons comprised 6.10+/-0.56% of the dLGN in VGlut2$^{flox/flox}$ animals and 7.84+/-1.73% in ET-33-Cre::VGlut2$^{flox/flox}$ animals (n=7 mice per genotype, $p>0.05$; Student's T-test). These data indicate that both the consolidation and maintenance of ipsilateral axon territory within the dLGN are largely insensitive to reductions in synaptic glutamate release both during and after eye-specific segregation -a finding that stands in bold contrast to current models of activity dependent retinogeniculate refinement (reviewed in Huberman et al., 2008a). Figure 2.10 provides a summary of our findings and compares them with studies in which retinal waves were altered.

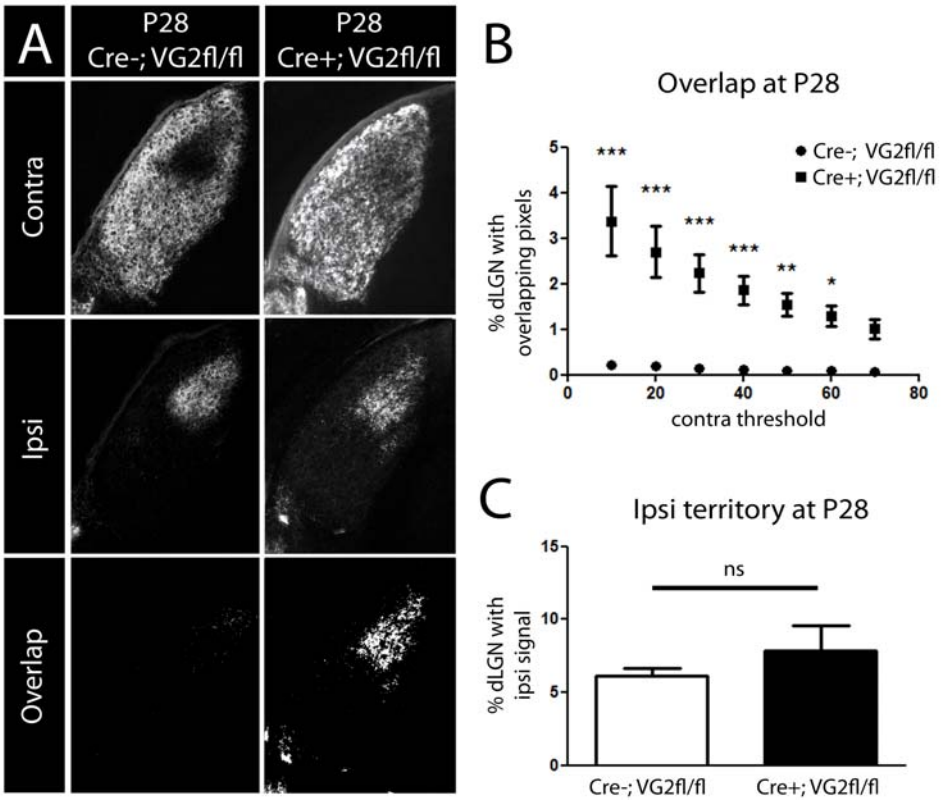

Figure 2.9 Maintenance of ipsilateral projections in the face of prolonged disruption of glutamatergic synaptic transmission. (A) Examples of retinogeniculate projection patterns at P28 in a Cre-:VGlut2$^{flox/flox}$ animal (left column) and a Cre+:VGlut2$^{flox/flox}$ littermate (right column). The Cre+ animal continues to exhibit contralateral axons (top row) throughout the entire dLGN, a robust ipsilateral projection (middle row), and a high degree of overlap (bottom). (B) Overlap at P28 (***p<0.001, **p<0.01, *p<0.05 by two-way ANOVA, n=7 per genotype). (C) Amount of ipsilateral signal at P28 (ipsi-eye axons occupied 6.10+/-0.56% of the dLGN in VGlut2$^{flox/flox}$ animals and 7.84+/-1.73% in ET-33-Cre::VGlut2$^{flox/flox}$ animals, n=7 mice per genotype, p>0.05).

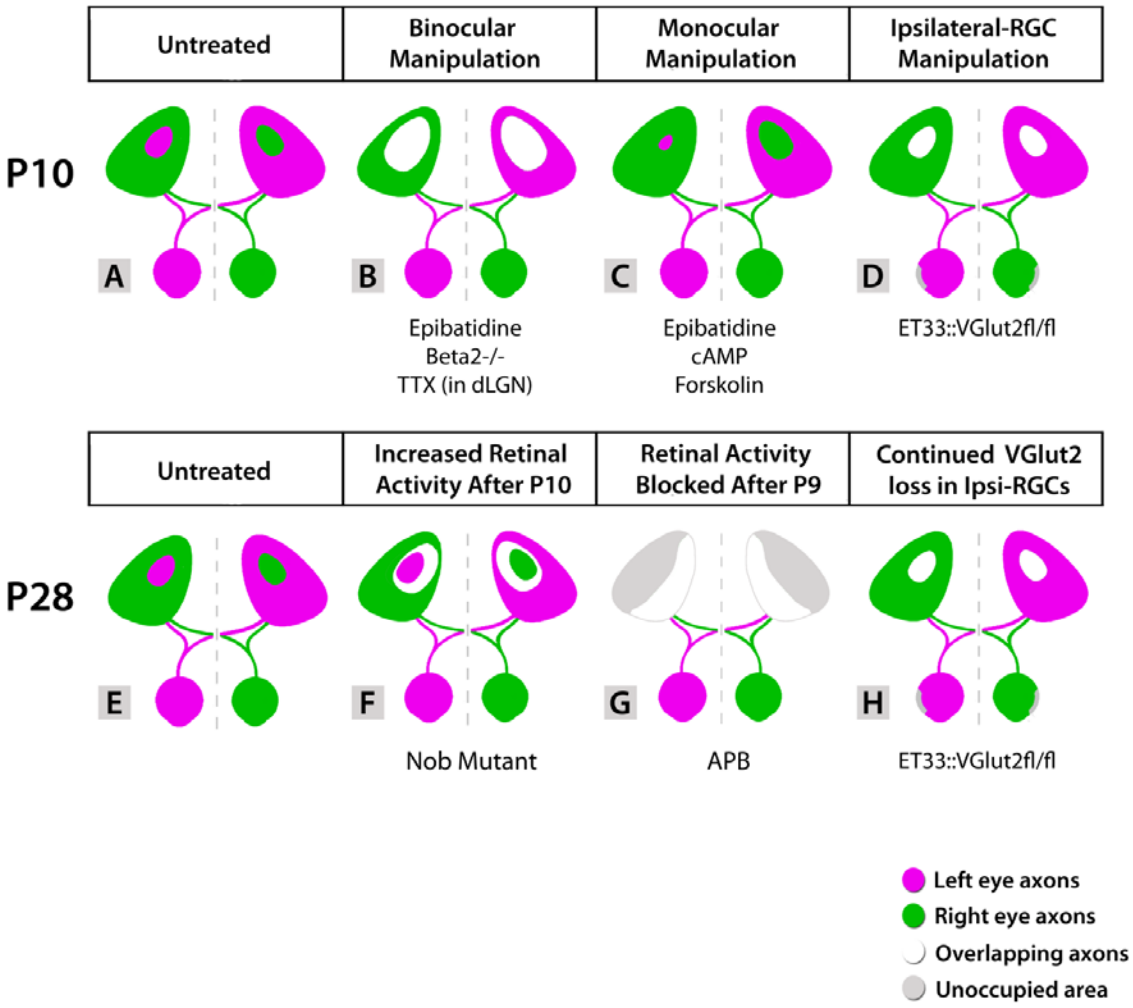

Figure 2.10 ET33-Cre::VGluT2$^{flox/flox}$ results compared to studies in which retinal waves were manipulated. (A) Normal P10 pattern. (B) Binocular activity disruptions that prevent axonal refinement (Huberman et al., 2002, 2003; Muir-Robinson et al., 2002; Penn et al., 1998; Rossi et al., 2001; Shatz and Stryker, 1988). (C) Monocular activity manipulations. For epibatidine experiments results reflect injection into the left (magenta) eye (Koch and Ullian, 2010; Penn et al., 1998). For the cAMP/forskolin experiments results reflect right eye (green) injection (Stellwagen and shatz, 2002). In each case the less active eye lost territory. (D) Results of the present study in which VGluT2 was selectively reduced in ipsilateral-projecting RGCs (in both eyes). (E) Normal pattern at P28. (F) Increased and persistent retinal activity causes expansion of ipsilateral territory in Nob mutants (Demas et al., 2006. (G) Retinal activity blockade after P9 caused ipsi axons to translocate into the contra-eye territory (Chapman, 2000). Experiment was performed in ferrets but is projected onto the mouse dLGN. (H) Results from the present study showing normal maintenance of ipsi-eye territory in the face of ongoing reduction of synaptic transmission at ipsilateral RGC-dLGN synapses. (A-H) White indicates overlap. Gray area is devoid of RGC axons.

2.2 Discussion

We found that reducing glutamatergic synaptic currents profoundly altered certain aspects of RGC axon remodeling whereas other aspects were unaffected. While reduced ipsilateral transmission led to an abnormal persistence of competing contra-eye axons in the ipsi-eye territory (Figure 2.6A,D), it did not prevent ipsi-eye axons from i) targeting to the appropriate region of the dLGN (Figure 2.6A), ii) refining into a normally sized termination zone (Figure 2.6A,E), and iii) maintaining that territory into the late postnatal period (Figure 2.9A,C). The ability of the release-deficient axons to consolidate and maintain their normal amount of target territory in the face of more active competing axons is surprising in light of previous studies (Chapman, 2000; Demas et al., 2006; Penn et al., 1998; Stellwagen and Shatz, 2002). The finding is, however, reminiscent of results from studies of cortical ocular dominance column development which demonstrated that early on, there is a strong functional bias in favor of contralateral eye connections and yet that bias does not prevent axons representing the ipsilateral eye from consolidating cortical territory (Crair et al., 1998; Crair et al., 2001).

An important caveat of our experimental manipulation is that it did not eliminate glutamate release completely. The present study, therefore, cannot determine if glutamate release is necessary for axon territory consolidation and maintenance. In addition, it is not presently possible to measure the effects of VGluT2 reduction on retino-dLGN transmission patterns in vivo; therefore, a full assessment of the synaptic defects present in ET33-Cre::VGluT2$^{flox/flox}$ mice during retinal waves remain to be determined. As it stands, the residual glutamate release observed in ET33::VGluT2$^{flox/flox}$ mice at P5 may be sufficient to stabilize and refine their ipsi-RGC axons, whereas the mechanism that eliminates competing axons may be more sensitive to alterations in glutamate release.

Why would ipsilateral axons refine normally with diminished VGluT2 (Figure 2.6) whereas monocular activity perturbations lead to a reduced ipsi-eye territory (Koch and Ullian, 2010; Penn et al., 1998)? The difference in those outcomes may reflect differences between

the experimental manipulations in the studies. While VGluT2 reduction weakened retinogeniculate transmission during eye-specific segregation (Figures 2.4 and 2.5), intraocular epibatidine treatment altered RGC spiking patterns (Penn et al., 1998; Sun et al., 2008) which in theory, should cause abnormal transmission patterns at retino-dLGN synapses. Abnormal patterns of synaptic activity may lead to a punishment signal that causes axons to be lost, whereas axons with dramatically weakened (or abolished) currents may fail to elicit or respond to such a signal. Another potential explanation is that in addition to evoking glutamate release from RGC axons, retinal waves cause calcium influxes in RGCs. Therefore, manipulations that alter spontaneous retinal activity patterns may exert broader effects on RGC axons than does VGlut2 reduction. A third possibility is that RGC axons may release factors other than glutamate to control the consolidation of their target territory, and those factors may be differentially impacted by epibatidine treatment versus VGluT2 reduction. For instance, RGCs express the vesicular monoamine transporter 2 (VMAT2) during development and the very promoter used to drive Cre expression in ipsi RGCs- SERT - is specifically expressed by ipsi-RGCs during development (Upton et al., 1999; Garcia-Frigola and Herrera, 2010). Indeed, eye-specific layers fail to form in animals lacking monoamine oxidase or SERT (Upton et al., 1999). In the future it will be interesting to address whether removal of SERT from VGluT2 depleted RGCs would disrupt their ability to consolidate and maintain dLGN territory.

In summary, our data demonstrate a key role for glutamatergic synaptic transmission during CNS circuit refinement in mediating the exclusion of axons from inappropriate target regions. However, contrary to what currents models of activity-dependent development would predict, our data also demonstrate that RGC populations with markedly reduced synaptic activity can still consolidate and maintain normal amounts of target territory, even in the presence of more active competitors. These findings advance our understanding of the mechanisms that establish developing CNS circuits by helping to clarify the direct contributions of glutamatergic synaptic transmission to axon refinement.

2.3 Materials and Methods

Mouse lines

The ET33 Sert-Cre transgenic mouse line was generated by GENSAT (Gong et al., 2007) and obtained from Mutant Mouse Regional Resource Centers (http://www.mmrrc.org/strains/17260/017260.html). Reporter lines: lox-STOP-lox-mGFP-IRES-NLS-LacZ-pA reporter (Hippenmeyer et al., 2005) was a gift from J.L. Rubenstein (UCSF), lox-STOP-lox-lacZ (Soriano, 1999) and lox-STOP-lox-tdTomato (Ai9; Madisen et al., 2009) were obtained from The Jackson Laboratory. Homozygous floxed VGlut2 mice were previously described (Hnasko et al., 2010). All mouse lines were congenic on the C57BL/6 background except for the mGFP mice which were maintained on a mixed 129SV/J and C57BL/6 background.

Retinal dLGN histology

Eyes were removed and fixed in 4% PFA for 1-2 hours at 4°C. Retinal whole mounts were prepared by extracting the retina from of the eye. Retinal sections were prepared by hemisecting the fixed eye, crypoprotecting it in 30% sucrose, freezing it and cryosectioning at 12µm. Preparation of dLGN tissue sections for histology: brains were removed and fixed overnight in 4% PFA at 4°C, followed by cryoprotection in 30% sucrose, and sectioning in the coronal plane at 40µm. Xgal staining: retinas were washed in buffer (0.0015M $MgCl_2$, .01% deoxycholate, .02% NP40, in phosphate buffer) 3 X 15min, then placed in stain (2.45mM x-gal in dimethylformamide, 5.0mM potassium ferrocyanide, 5.0mM potassium ferricyanide, in wash buffer) for 2 hours at 37ºC, and washed again 3 X 15min. To visualize the mGFP reporter immunostaining for GFP was performed as described (Huberman et al., 2008b). Imaging of the tdTomato reporter did not require immunostaining.

Retinal cell culture and immunohistochemistry

Retinas were harvested from P3 mice, digested in a papain solution (16.5 U/ml; Worthington), mechanically dissociated to form a cell suspension, and plated on glass coverslips (coated with 10mg/ml poly-d-lysine and 2mg/ml laminin) at a concentration of 25,000 cells per well in a 24-well plate. Cells were incubated in defined media (Meyer-Franke et al., 1995) including growth factors (Goldberg et al., 2002). Reagents were purchased from Sigma.

At DIV2, cultured retinal cells were fixed in 4% paraformaldehyde, rinsed in PBS, and blocked at room temperature for 30 minutes in a 1:1 mix of goat serum and antibody buffer (150 mM NaCl, 50 mM tris base, 1% L-lysine, 0.4% azide). The cells were incubated in guinea pig anti-Vglut2 polyclonal antibody (1:1500, Millipore) overnight at 4°C then rinsed in PBS (3X 10 minutes). Cells were then incubated in Alexa Fluor 488 goat anti-guinea pig antibody (1:500, Invitrogen) at room temperature for 1.5 hours followed by three rinses in PBS. Vectashield was used for mounting coverlsips onto microscope slides.

Cells were imaged at 20x using a Zeiss Axio Imager.M1 microscope. All images were imported into Adobe Photoshop and thresholded. ET33-Cre expressing cells were identified by their expression of tdTomato reporter protein. The somas of the Cre-expressing cells were outlined and the average fluorescence intensity of the Vglut2 signal within the traced area was measured using the histogram function. VGlut2 fluorescence intensity was normalized to soma size for each cell. A Student's t-test was used to compare VGlut2 fluorescence intensity between genotypes (ET33-Cre::VGlut2$^{+/+}$ and ET33-Cre::VGlut2$^{flox/flox}$).

Electrophysiology

For electrophysiological analysis one retina was removed on either P0 or P5 and recordings were performed on P5 or P10. Mice were anesthetized with isofluorane and one eye was removed or in some cases a slit was made across the cornea through which the lens and retina were removed.

Brain sections (325μm) containing both the optic tract and dLGN were acutely prepared as previously described (Chen and Regehr, 2000; Koch and Ullian, 2010; Bickford et al., 2010). Sectioning was performed in oxygenated cutting solution consisting of (in mM): 78.3 NaCl, 23.0 $NaHCO_3$, 23.0 Dextrose, 33.8 Choline Chloride, 2.3 KCl, 1.1 NaH_2PO_4, 6.4 $MgCl_2$, 0.45 $CaCl_2$. Brains were incubated for 25 min at 34°C brains in cutting solution then transferred to oxygenated ACSF consisting of (in mM): 125.0 NaCl, 25.0 $NaHCO_3$, 25.0 Dextrose, 2.5 KCl, 1.25 NaH_2PO_4, 2.0 $CaCl_2$, 1.0 $MgCl_2*6H_20$. Recordings were made at room temperature. Whole-cell voltage-clamp recordings of dLGN neurons were obtained using 2.5-3.5MOhm patch electrodes containing an internal solution consisting of (in mM): 35 CsF, 100 CsCl, 10 EGTA, and 10 HEPES. Inhibitory inputs were blocked with 20μM bicuculline methobromide (Tocris). Recordings were sampled at 10-20kHz and filtered at 1kHz. Access resistance was monitored throughout the recording period and was adjusted to 4-9MOhms after 70% compensation. A concentric bipolar stimulating electrode was placed just touching the surface of the optic tract next to the ventral LGN, and a 1ms stimulus was delivered every 30 seconds. A 40μA stimulus was used since this intensity evoked action potentials from many RGC axons, typically resulting in maximal postsynaptic responses in control cells. NMDAR-mediated current amplitudes were measured at a holding potential of +40mV by evoking synaptic currents and measuring the peak of the current trace at a time when the AMPAR-mediated currents no longer contributed to the response, ~25ms after the onset of the EPSC. Synaptic currents were analyzed using Igor Pro, Microsoft Excel, and GraphPad Prism software programs. All experiments and analyses were done blinded to genotype. Throughout this paper statistical comparisons were made using a Student's unpaired t-test unless otherwise stated.

Dye-labeling retinogeniculate axons

Mice were anesthetized with isoflurane and fused eyelids were gently separated with tweezers. Eyes were numbed with proparacaine and injected with 1.0-3.0μL of CTb-488 or CTb-594 (0.5% in sterile saline) (1.0 μL for P3 mice, 2.0 μL for P9 mice, and 3.0 μL for P27).

Analysis of retinogeniculate projections

Confocal images of dLGN sections were acquired using an Axiovert 200 Microscope and Pascal acquisition software. Images were imported into Adobe Photoshop and binarized using a threshold that corresponded to a location in the grayscale histogram where there was a clear distinction between the CTb label and background fluorescence signals. Thresholded images were imported into ImageJ and the boundary of the dLGN was delineated in order to exclude label from the optic tract and intrageniculate leaflet. The area occupied by the ipsilateral axons was measured by selecting all ipsi signal-containing pixels within the dLGN and comparing this measurement to the total number of pixels within the dLGN. For measurements of binocular overlap the binarized ipsi and contra images were first multiplied in photoshop (yielding images containing only the overlapped signal) and then imported into ImageJ for analysis of the amount of overlapping signal within the dLGN. In addition, analysis of axonal overlap was performed over a range of signal-to-noise thresholds (Bjartmar et al., 2006; Rebsam et al., 2010; Torborg et al., 2005). Two sections from the center of the dLGN on both sides of the brain were averaged for each animal.

Chapter 3

Neuronal pentraxins mediate silent synapse conversion in the developing visual system

This chapter contains our completed manuscript that was published in the Journal of Neuroscience.

3.1 Introduction

AMPA receptor recruitment is necessary to confer functionality to newly-formed excitatory synapses and is a requirement for normal brain function; however, the mechanisms underlying the development of AMPAR signaling at nascent synapses remain controversial (Voronin and Cherubini, 2004; Xiao et al., 2004). Among the molecules hypothesized to act as early mediators of synaptic AMPAR recruitment are the neuronal pentraxins. This family consists of three members, NP1, NP2 (also known as neuronal activity-regulated protein or Narp), and NPR (neuronal pentraxin receptor). NPR is an integral membrane protein while NP1 and NP2 are secreted molecules, and the three form heteromultimers in which NP1 and NP2 can be tethered to the membrane through NPR (Kirkpatrick et al., 2000). NPs are multifunctional proteins expressed specifically at excitatory synapses throughout the brain. Recent evidence indicates that one member of this family, NPR, is required for mGluR1/5 dependent LTD (Cho et al., 2008). In contrast, NP1 and NP2 and are thought to act trans-synaptically to cluster AMPARs at postsynaptic sites and to promote excitatory synaptogenesis (O'Brien et al., 1999; O'Brien et al., 2002; Reti et al., 2002; Xu et al., 2003; Sia et al., 2007). In support of this, the C-terminal domain of NPs has been shown to interact with the N-terminus of glutamate receptor subunits (Xu et al., 2003; Sia et al., 2007), and overexpression of NPs in cultured presynaptic neurons caused enhanced postsynaptic AMPAR clustering (O'Brien et al., 1999; O'Brien et al., 2002). In addition, expression of dominant negative NP2 *in vitro* reduces GluR1 clustering along dendrites of cultured spinal neurons (O'Brien et al., 2002), and both knockdown and knockout of NPs were shown to reduce GluR4 clustering on hippocampal neurons (Sia et al., 2007). Despite this compelling evidence supporting a developmental role

for NPs in synaptic AMPAR recruitment, a physiological function for NPs at nascent synapses *in vivo* has not been established (Bjartmar et. al., 2006).

Here we investigate the function of NP1 and NP2 at retinogeniculate synapses in the developing mouse visual system. NP1/2 are expressed in retinal ganglion cells (RGCs) and in the visual thalamus where they are required for the eye-specific refinement of RGC axons during early postnatal life (Bjartmar et al., 2006); thus, NP1/2 are important molecules in this system during *in vivo* development. In addition, RGCs cultured from NP1/2 KO mice displayed a pronounced delay in the development of synaptic AMPAR-mediated currents (Bjartmar et al., 2006). These data suggested that NP1/2 might participate in the development of AMPAR-mediated currents at native retinogeniculate synapses, and that deficits in synaptic physiology could contribute to the failure of NP1/2 KO axons to segregate normally. Here we use acute slice physiology to characterize the role of NP1/2 at native retinogeniculate synapses over development. In addition, because NP1/2 KO mice displayed physiological phenotypes both in the retina and in the dLGN we used *in vivo* retinal activity manipulations and axon labeling to investigate the role of retinal activity in axon remodeling in NP1/2 KO mice.

3.2 Results

In the rodent dLGN, the bulk of synaptogenesis occurs over the first week of postnatal life and it is during this time that AMPAR-mediated currents can first be recorded from retinogeniculate synapses (Ziburkus and Guido, 2006). This period also corresponds to the peak of NP1/2 expression in this system (Bjartmar et al., 2006). Therefore, to assess the role of NP1/2 in the development of retinogeniculate synaptic function we recorded from dLGN neurons in acutely prepared brain slices between the ages of postnatal day 6 and 9 (P6-P9), when AMPAR-mediated currents could be reliably detected in all WT dLGN neurons. Slices containing the dorsal lateral geniculate nucleus (dLGN) and the optic tract were prepared using the method of Chen and Regehr, which preserves the retinal inputs to the nucleus (Chen and Regehr, 2000). Optic tract stimulation was used to evoke transmission at retinogeniculate synapses and thalamic neurons were voltage clamped at either -70mV or +40mV to measure

AMPAR-mediated and NMDAR-mediated currents, respectively. As is characteristic of early retinogeniculate transmission, this method produced robust evoked NMDAR-mediated currents and somewhat weaker AMPAR-mediated currents, and varying the stimulus intensity showed that the immature relay neurons were multi-innervated (Figure 3.1A,B). Indeed all parameters of evoked WT transmission reported below are in good agreement with previous studies (Chen and Regehr, 2000; Liu and Chen, 2008).

Like WT neurons, neurons from NP1/2 heterozygous animals (NP1/2 Hets) and neurons from NP1/2 KO animals also displayed robust NMDAR-mediated evoked responses (Figure 1A,B). However, in contrast to WTs and NP1/2 Hets, we observed little to no AMPAR-mediated transmission in recordings from NP1/2 KO neurons (Figure 3.1A,B). When relay neurons were voltage clamped at -70mV and a maximal stimulus was delivered to the optic tract, the peak amplitudes of the AMPAR-mediated responses were severely reduced in NP1/2 KO neurons compared to WT and NP1/2 Het neurons (Figure 3.1C, WT=-244.20+/-31.97pA, Het=-209.95+/-42.32pA, KO=-80.86+/-19.48pA; WT,KO $p<0.05$, Het,KO $p<0.05$ by one-way ANOVA followed by Bonferroni's multiple comparisons test). The AMPA/NMDA ratio, a measure of the relative strength of the two components of the evoked response, was also decreased in NP1/2 KO neurons (Figure 3.1D, WT=0.44+/-0.07, Het=0.36+/-0.04, KO=0.14+/-0.03; WT,KO $p<0.05$, Het,KO $p<0.05$ by one-way ANOVA followed by Bonferroni's multiple comparisons test). The reduced ratio reflected a specific deficit in the AMPAR-mediated currents since neither the average amplitude (Figure 3.1C, WT=636.76+/-129.98pA, Het=658.20+/-115.49, KO=657.97+/-93.81pA; WT,KO $p>0.05$, Het,KO $p>0.05$) nor time course (WT=194.48+/-16.66, Het=220.92+/-9.27, KO=209.30+/-19.55; WT,KO $p>0.05$, Het,KO $p>0.05$) of the NMDAR-mediated responses were affected by NP1/2 knockout (one-way ANOVA followed by Bonferroni's multiple comparisons test). We reasoned that this specific reduction in AMPAR-mediated transmission with no accompanying change in NMDAR-mediated transmission was likely to have a postsynaptic origin and we tested this using a common measure of presynaptic release probability, the paired pulse ratio (PPR). Since the NP1/2 KO AMPAR-mediated currents were

small and sometimes absent we analyzed the PPR of the NMDAR-mediated currents. In this and subsequent experiments we focused on WT and KO neurons since heterozygous neurons displayed synaptic currents that were indistinguishable from WTs. PPRs were measured at 5 different inter-stimulus intervals (50, 100, 200, 500, and 1000ms) and no differences were found between WT and KO PPRs at any of these intervals (Figure 3.1E,F, two-way ANOVA followed by Bonferroni post tests), suggesting that presynaptic release is not reduced by the loss of NP1/2. Taken together, these data demonstrate that the absence of NP1/2 during *in vivo* development leads to a specific deficit in AMPAR-mediated transmission at newly-formed synapses.

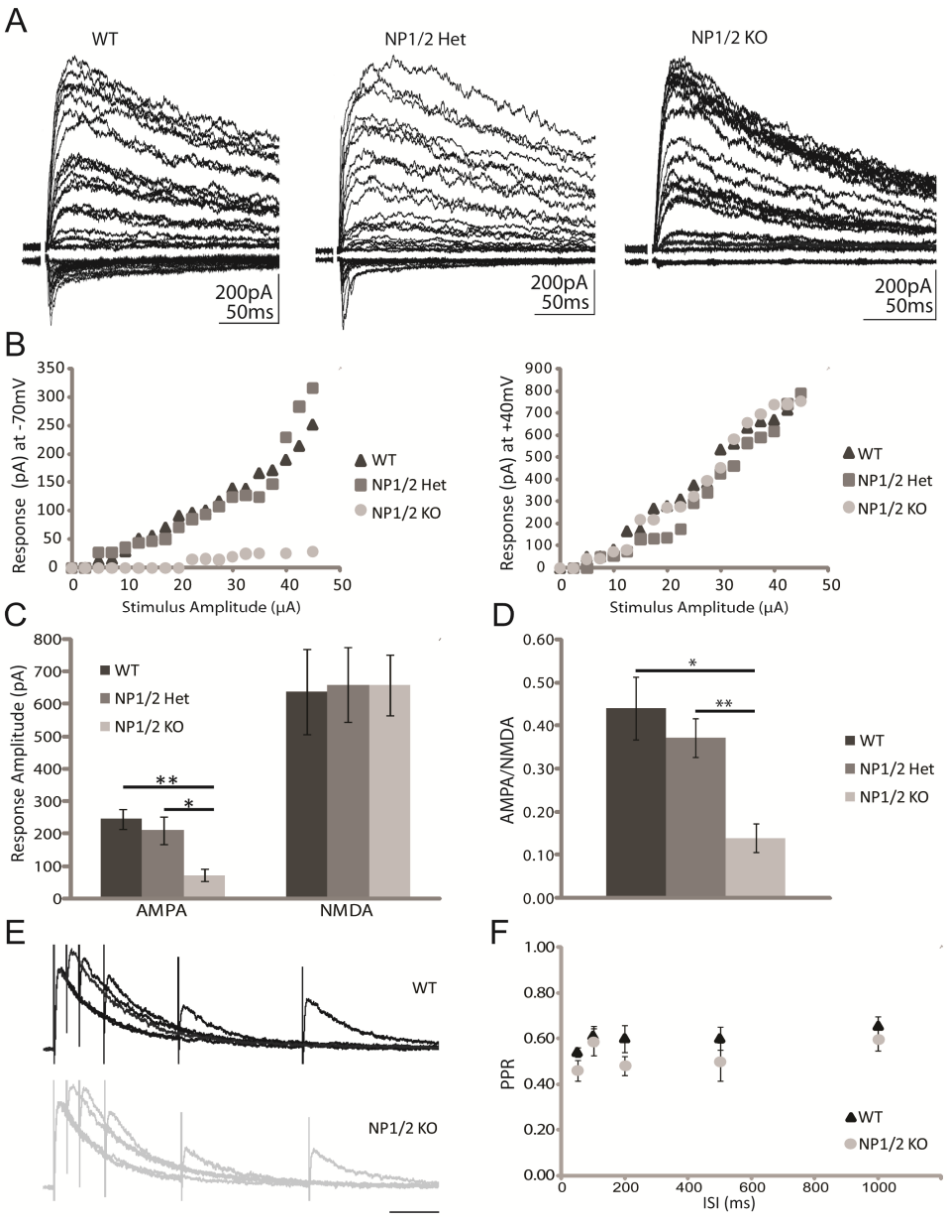

Figure 3.1 NP1/2 knockout neurons have a specific deficit in AMPAR-mediated synaptic transmission during early postnatal development (P6-P9). (**A)** Example traces from WT, NP1/2 Het, and NP1/2 KO dLGN neurons voltage clamped at -70mV and +40mV. The optic tract was stimulated over a range of stimulus intensities. **(B)** Input-output curves showing EPSC amplitude as a function of stimulus intensity. (**C)** Average amplitudes of maximal AMPAR and NMDAR currents. (**D)** Average AMPA/NMDA ratios. (**C-D)** n=9 WT animals (26 cells), 6 NP1/2 Het animals (15 cells), and 6 NP1/2 KO animals (26 cells). Data compared with student's t-test. *p<0.05, **p<0.01 **(E)** Example traces from a WT neuron (upper) and an NP1/2 KO neuron (lower) voltage clamped at +40mV and stimulated with pairs of pulses at 5 different inter-stimulus intervals (50, 100, 200, 500, and 1000ms). **(F)** Average PPRs for WTs (3 animals, 8 cells) and NP1/2 KO neurons (2 animals, 4 cells) over the 5 ISIs tested.

In the NP1/2 KO mouse RGC spiking was shown to be increased during early postnatal life (Bjartmar et al., 2006) raising the possibility that the severely reduced AMPAR-mediated currents in the KO dLGN could be due to altered retinal activity instead of to the loss of NP1/2 from retinogeniculate synapses (Shah and Crair, 2008a). To begin to distinguish between these possibilities we pharmacologically enhanced RGC spiking in WT animals *in vivo* and subsequently measured retinogeniculate currents to determine if increased retinal activity can lead to diminished retinogeniculate transmission. Binocular injections of the cyclic AMP analogue, CPT-cAMP, were used to enhance RGC spiking since this treatment has been previously demonstrated to increase RGC activity in WT animals through enhancing presynaptic drive from cholinergic amacrine cells (however, we did not verify the effects of cAMP in this study) (Stellwagen et al., 1999). Retinal activity was increased for three to four days between the ages of P4 and P7-P8 via repeat intraocular injections performed 48 hours apart. Retinogeniculate currents were assessed on P7 and P8. No difference in retinogeniculate transmission was observed between CPT-cAMP and saline-treated animals (Figure 3.2). This finding shows that increased retinal spiking, per se, does not reduce AMPAR-mediated transmission at retinogeniculate synapses, which is consistent with a direct role for NP1/2 in retinogeniculate transmission. However, it remains possible that the unique features of retinal waves altered in the NP1/2 KOs might contribute to synaptic AMPAR-mediated recruitment.

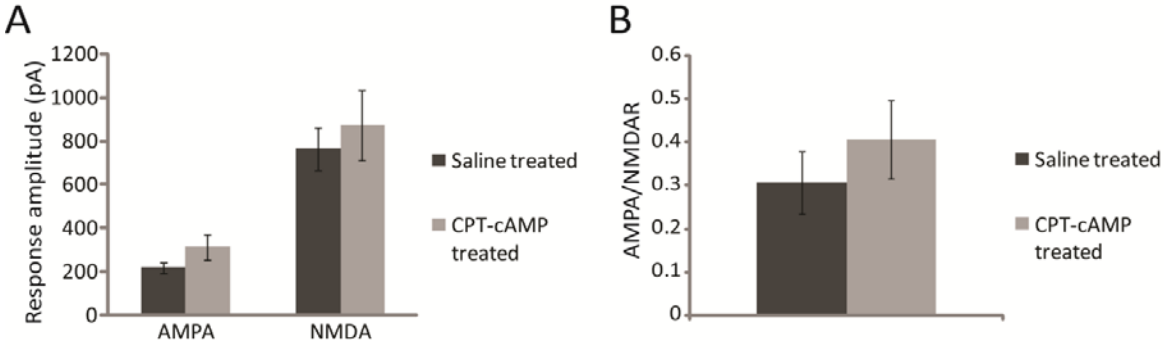

Figure 3.2 Increased retinal activity *in vivo* over multiple days (P-P7/8) does not lead to reduced retinogeniculate transmission. **(A)** Average peak amplitudes of AMPAR and NMDAR-mediated retinogeniculate responses from control-treated and CPT-cAMP-treated animals. **(B)** Average AMPA/NMDA ratios. **(A,B)** Dataset included 5 animals (17 cells) treated with CPT-cAMP and 2 saline-treated animals (11 cells). No significant differences were found.

What synaptic mechanisms might account for the reduced AMPAR-mediated currents in NP1/2 KO neurons? Because neuronal pentraxins have been reported to cluster glutamate receptors at hippocampal and spinal synapses (O'Brien et al., 1999; O'Brien et al., 2002; Xu et al., 2003; Sia et al., 2007), we hypothesized that the decrease in AMPAR-mediated transmission was due to the presence of fewer AMPARs clustered at retinogeniculate synapses. To test this we measured quantal size, which should be reduced in NP1/2 KO neurons if each synapse contains fewer AMPARs. Because dLGN neurons receive excitatory input from both retinal and cortical inputs it is impossible to know the origin of spontaneously released vesicles; consequently, we used optic tract stimulation to evoke quantal events specifically at retinogeniculate synapses. This was accomplished by replacing extracellular calcium with strontium, which promotes the asynchronous release of synaptic vesicles (Miledi, 1966). Accordingly, we found that strontium both reduced the EPSC (Figure 3.3A, arrows) and allowed for the resolution of unitary events (Figure 3.3A, asterisks) at a frequency that was 5.9-fold greater than the background rate (event frequency without stimulation compared to the frequency measured during the first 300ms after stimulation). This suggests that about 83% of the analyzed events were evoked from RGC synapses while the remaining 17% were a mixed population arising from both retinal and cortical inputs; therefore, at least 83% of the events occurred at retinogeniculate synapses. While the initial responses were greatly reduced in NP1/2 KO neurons compared to WT neurons (Figure 3.3A), the average size of the quantal events did not differ between the genotypes (Figure 3.3B shows example traces; average quantal size for WTs and NP1/2 KOs were -9.49+/-0.42pA and -9.89+/-0.64pA, respectively; $p>0.05$). Since quantal size at young retinogeniculate synapses is quite small (Chen and Regehr, 2000) decrements in quantal size may be difficult to detect since reduced events could fall into the noise. To address this issue we first confirmed that the baseline signals did not differ between the WT and NP1/2 KO recordings by comparing their average standard deviations (WT=2.76+/-0.30pA, NP1/2 KO=2.71+/-0.33pA; $p>0.05$). To then determine if the two populations of event amplitudes differed in profile we analyzed the cumulative probability of event amplitudes using 1pA bins (Figure 3.3C). If the loss of NP1/2 leads to many quantal

events falling below the detection limit then we would expect this distribution to be left-shifted; however, the distributions were very similar in profile and were not statistically different from one another (Kolmogorov-Smirnov test P>0.05). These surprising data strongly suggest that reduced quantal size does not underlie the deficit in AMPAR-mediated transmission in NP1/2 KO neurons.

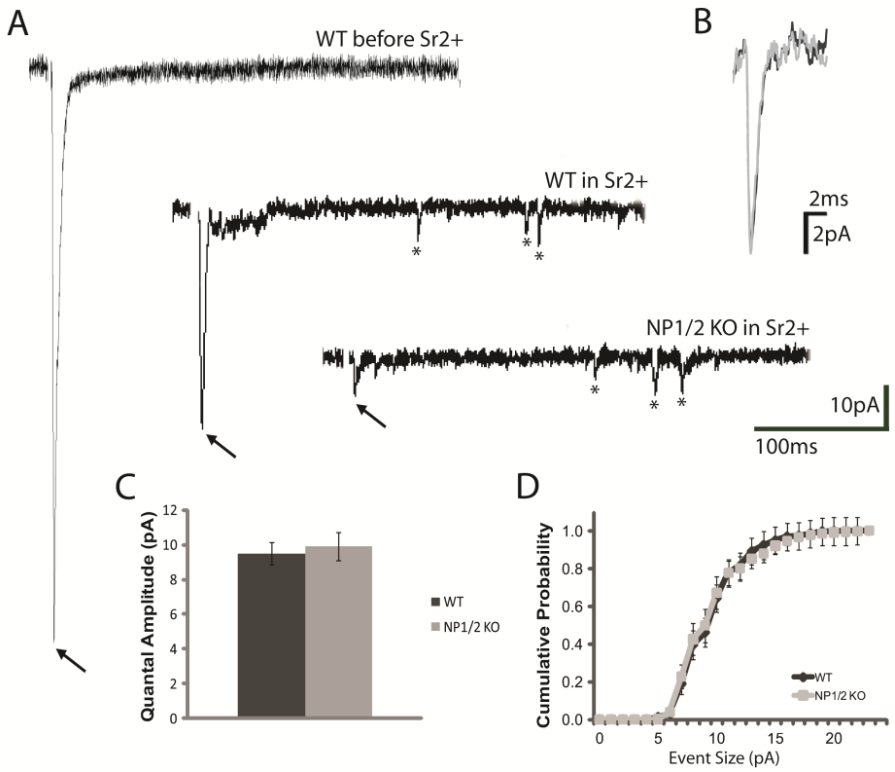

Figure 3.3 Quantal size is not reduced in NP1/2 KOs (P6-P9). (**A)** Examples of evoked responses in the absence and presence of Sr^{+2}. Top left shows a WT recording in Ca^{+2} external. Middle trace shows WT response in Sr^{+2} external. Bottom right trace shows NP1/2 KO response in Sr^{+2}. An initial fast response (arrows) was followed by delayed release of quantal events (asterisks). (**B)** Overlay of the average mEPSCs from a WT neuron (black) and an NP1/2 KO neuron (gray). **(C)** Average cumulative probability histograms. Distributions were not different by a K-S test. N=4 WT mice (13 cells) and 3 KOs (10 cells).

If quantal size is unaltered in NP1/2 KO neurons what accounts for their diminished AMPAR-mediated currents? One possibility is that loss of NP1/2 results in fewer AMPAR-containing synapses, that is, an increased number of silent synapses. Analysis of the currents arising from the stimulation of presumably single retinal fibers has previously provided evidence for silent synapses at this developing connection (Chen and Regehr, 2000; Liu and Chen, 2008). Early in development individual retinal inputs form relatively few AMPAR-containing synapses with dLGN neurons; therefore, sometimes all the synapses associated with an individual retinal input are silent. These silent inputs can be detected using the protocol of Chen and Regehr (2000) in which reduced stimulus intensity is used to presumably activate just one retinal axon. Based on these studies, a retinal input is considered silent when this stimulus, which produces the smallest reliable NMDAR-mediated response when held at +40mV, fails to elicit an AMPAR-mediated current when the neuron is held at -70mV. We compared the number of these silent inputs observed in the WT and NP1/2 KO populations as an indicator of the relative abundance of silent synapses present on WT and KO neurons (Figure 3.4). Using this protocol most WT neurons responded when held at either +40mV or -70mV; however, 38% (9 out of 24) showed no AMPAR-mediated current creating a bimodal histogram of response amplitudes at -70mV (Fig. 3A,C). In contrast, most NP1/2 KO neurons had detectable responses only at +40 mV with 69% (18 of 26) showing no AMPAR-mediated current; therefore, NP1/2 KO neurons had about twice as many silent inputs as WT neurons (Figure 3.4A,D). Since single fiber stimulation either did or did not result in a postsynaptic response at -70mV we employed the binomial test to determine if the probability of failure was higher in the NP1/2 KOs compared to WTs. We found that, given the probability of failure in the WT population, the likelihood of obtaining the specific distribution of responses and failures that was observed in the NP1/2 KO population (that is, 8 responses and 18 failures) was 0.0003, a highly significant reduction from WT ($p<0.001$).

Since there are twice as many silent inputs in the NP1/2KOs compared to the WTs this suggests that KO neurons have at least twice as many silent synapses as WT neurons, and the average amplitudes of the successful single fiber responses recorded at -70mV were in good agreement with this interpretation. On average the single fiber responses of the KOs at -70mV were about half the size of the single fiber WT responses (Figure 3.4B, WT=-31.06+/-4.03pA, NP1/2KO=-16.29+/-0.78pA; $p<0.01$). Similarly, the average AMPA/NMDA ratios were also reduced in NP1/2 KO neurons (WT=0.44+/-0.12, KO=0.13+/-0.05; $p<0.05$). In WT animals the average quantal response at this age is -9.49pA and the average single fiber response is -31.06pA suggesting that a typical WT RGC forms ~3 fully-functional, AMPAR-containing synapses with a given WT dLGN neuron. In contrast, the average quantal and single fiber responses of the NP1/2 KOs were -9.89pA and -16.29pA, respectively, suggesting 1.5 AMPAR-containing synapses per RGC input; a reduction of about one half. Finally, the average single fiber responses at +40mV were identical between WTs and KOs (Figure 3.4B,D, WT=54.49+/-7.06, NP1/2KO=61.20+/-10.07, $p>0.05$). Because both the maximal and presumed single fiber NMDAR-mediated responses were the same for WTs and KOs this suggests that the total number of synapses formed between individual RGCs and dLGN neurons was not altered by the loss of NP1/2 (Chen and Regehr, 2000). Based on these data we conclude that the deficit in synaptic transmission in the NP1/2 KO animals is most likely due to an increased number of synapses lacking functional AMPARs. These surprising findings suggest a novel role for NP1/2 in silent synapse conversion during early postnatal development; however, they do not rule out the possibility that NP1/2 may modulate the functional properties of AMPARs.

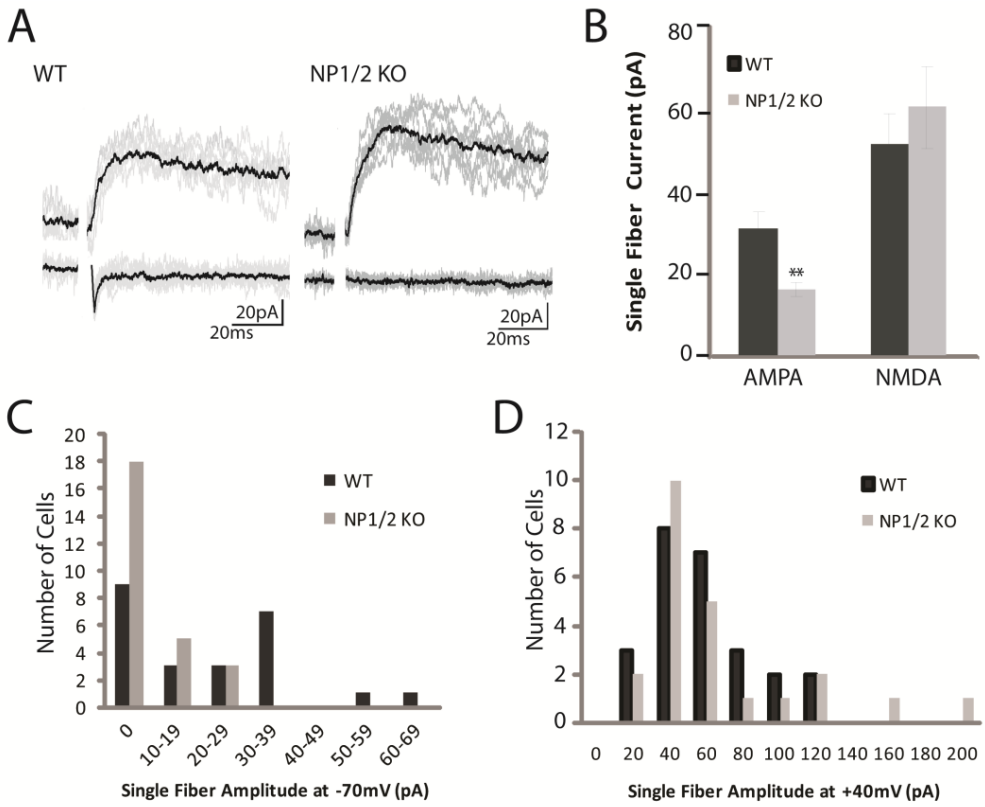

Figure 3.4 Young NP1/2 KO dLGN neurons (P6-P9) have an increased number of silent synapses. (A) Example traces from WT (left) and NP1/2 KO (right) neurons at +40 and -70 mV showing responses to minimal stimulation (7.5μA for both cells). WT neuron shows responses at both +40 and -70 mV while NP1/2 KO neuron shows a response only at +40 mV. **(B)** Average amplitudes of presumed single fiber responses at -70mV and +40mV. **(C)** Histogram of single fiber responses of WT and NP1/2 KO neurons held at -70 mV. Note the increase in the number of NP1/2 KO neurons that showed no response. **(D)** Histogram of single fiber responses of WT and NP1/2 KO neurons held at +40 mV. **(B-D)** Data displayed as mean+/-SEM. **p<0.01. Data set included 24 cells from 8 animals for WTs and 26 cells in 6 animals for KOs.

In WT mice AMPAR-mediated responses at retinogeniculate synapses strengthen dramatically between P10 and P30, which leads to about a 5-fold increase in the AMPA/NMDA ratio and shifts retinogeniculate transmission from being NMDAR to AMPAR-dominated (Chen and Regehr, 2000). To determine if this characteristic phase of synaptic strengthening is prevented in the absence of NP1/2 we measured synaptic transmission during this period, between the ages of P17 and P20. At this later age we found robust AMPAR-mediated responses in both WT and NP1/2 KO neurons (Figure 3.5A) with AMPA/NMDA ratios that no longer differed between the two groups (WT=1.17+/-0.21; KO=1.53+/-0.29; p>0.05), indicating

that at this age NP1/2 are no longer required for the strengthening of AMPAR-mediated transmission. Although these data do not rule out a role for NP1/2 in the strengthening of AMPAR-mediated transmission later in development, they highlight the importance of NP1/2 at immature synapses since at this early stage retinogeniculate synapses cannot easily compensate for the loss of NP1/2.

A surprising aspect of our P17-P20 recordings was that although the AMPA/NMDA ratios of NP1/2 KO neurons were not significantly different from WTs, the absolute amplitudes of both the AMPAR and NMDAR-mediated currents were increased in NP1/2 KO neurons compared to WT neurons (Figure 3.5B, WT AMPA=-1102.92.08+/-173.16 and NMDA=1057.03+/-220.92pA; KO AMPA=-2993.84+/-535.27 and NMDA=1900.29+/-184.48; $p<0.05$ for both current components). We next asked whether an increase in the strength of individual inputs might be contributing to the enhanced maximal KO currents. Using minimal stimulation to measure the currents arising from presumably single fibers we found that WTs and KOs did not differ in the amplitudes of their presumed single fiber AMPAR-mediated currents (Figure 3.5C,D; WT=-195.77+/-53.86, NP1/2KO=-193.13+/-73.80; $p>0.05$), the amplitude of their single fiber NMDAR-mediated currents (Figure 3.5C,D; WT=184.33+/-84.64, NP1/2KO=144.27+/-25.22; $p>0.05$), or in their AMPA/NMDA ratios (WT=1.16+/-0.18, NP1/2KO=1.46+/-0.49; $p>0.05$).

Since the presumed single fiber currents were not increased in the KOs this suggests that enhanced presynaptic release may not contribute to their excessive total synaptic drive; however, to investigate the contribution of altered release probability to the aberrantly large synaptic currents in the KOs we measured the paired pulse ratios of P17-P20 WT and NP1/2 KO neurons. Using an ISI of 100ms and found that there was no difference between the two groups when recorded at either -70mV in the presence of cyclothiazide to eliminate the effects of AMPAR desensitization (Chen and Regehr, 2003) (Figure 3.5E,F, WT=0.50+/-0.06; KO=0.51+/-0.09; $p>0.05$) or at +40mV (Figure 3.5F, WT=0.51+/-0.05, NP1/2KO=0.49+/-0.06; $p>0.05$). These findings suggest that enhanced presynaptic release does not account for the increased synaptic currents in the NP1/2 KOs.

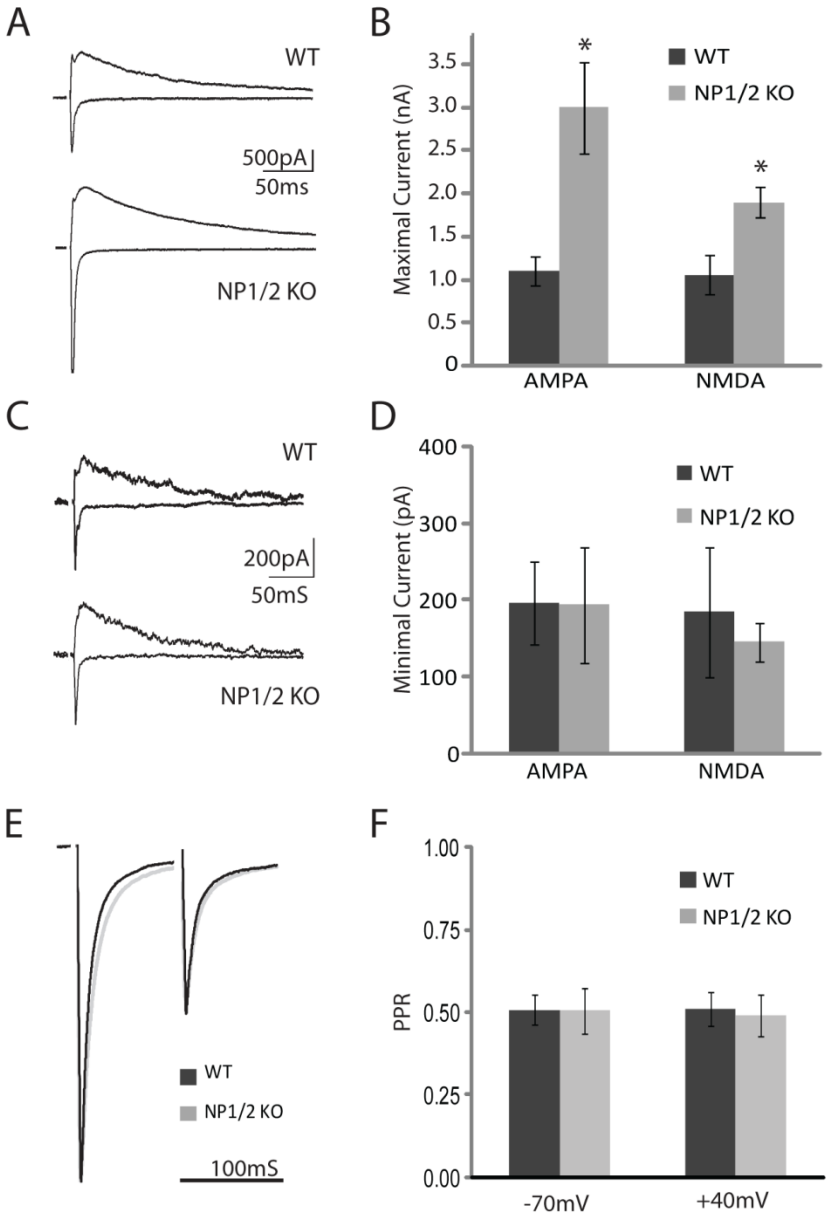

Figure 3.5 P17-P20 NP1/2 KO animals strengthen AMPAR-mediated currents by an NP1/2-independent mechanism and develop aberrantly large current amplitudes. (**A)** Example traces at +40mV and -70mV from WT and NP1/2 KO neurons at age P19 showing maximal evoked responses (50μA stimulus). (**B)** Average saturating AMPAR and NMDAR-mediated responses. (**C)** Example traces of presumed single fiber responses from a WT neuron (10μA stimulus) and a KO neuron (7.5μA stimulus) recorded at +40mV and -70mV. (**D)** Average minimal AMPAR and NMDAR-mediated responses. **(B,D)** Data displayed as mean+/-SEM. For WTs n=8 animals and 17 cells. For KOs n=9 animals and 17 cells. *p<0.05 **(E)** Examples of PPRs at -70mV in cyclothiazide. **(F)** Quantification of PPRs recorded at -70mV and +40mV. For -70mV recordings n=3 WT animals (8 cells) and n=2 KO animals and 6 cells. For +40mV recordings n=2 animals 4 cells for both genotypes. Data displayed as mean+/-SEM.

Since the maximal currents were enhanced in the KOs while their single fiber currents were unchanged, this suggests individual dLGN neurons may be innervated by an increased number of RGC axons. While AMPAR-mediated transmission is dramatically strengthened at "winning" retinogeniculate synapses between P10 and P30, another prominent feature of this phase of retinogeniculate development is the removal of inappropriate functional connections. This phase is often referred to as "within-eye segregation" since eye-specific segregation is largely completed but dLGN neurons are still refining excessive inputs originating from the same eye. During this period the number of RGC inputs onto individual dLGN neurons is reduced from around a dozen to just one or two (Chen and Regehr, 2000; Ziburkus et al., 2003). Because both synaptic maturation and eye-specific segregation are severely delayed in the NP1/2 KOs (Bjartmar et al., 2006), we reasoned that within-eye segregation might also be delayed in the absence of NP1/2 leading to more highly innervated dLGN neurons. Two methods were used to determine whether P17-P20 NP1/2 KO neurons might receive input from a greater number of RGCs than WT neurons. First, we divided the maximal currents by the minimal currents in order to estimate the number of inputs received by individual dLGN neurons. This method suggested that on average WT neurons between the ages of P17 and P20 receive roughly 4 to 5 inputs (Figure 3.6, input number = 4.71+/-1.80 and 4.94+/-1.91 when neurons were held at -70mV and +40mV, respectively), an estimate similar to previous reports (Hooks and Chen, 2006). In contrast, NP1/2 KO neurons were estimated to receive input from around a dozen RGCs, a significant increase (Fig. 3.6, input number = 12.99+/-5.64 at -70mV and 13.14+/-3.58 at +40mV; $p<0.05$ for both).

To gain further evidence regarding whether input elimination might be aberrant in the NP1/2 KOs we counted functional inputs onto dLGN neurons using a common method in which the stimulus amplitude is adjusted to elicit a single fiber response and then gradually increased in order to systematically recruit all additional inputs to the neuron (Figure 3.6A) (Chen and Regehr, 2000). The visibly discernable "steps" in the current traces were counted and cells were characterized by sorting them into three categories: "refined" cells had just one or two

large inputs, “resolving” cells had three to six easily discernable inputs, and “unrefined” cells had more than six inputs with current steps that were less well separated (Hooks and Chen, 2006; Stevens et al., 2007). Inputs were counted blind to genotype to prevent experimenter bias. At this age, dLGN neurons are in the process of becoming refined and they typically receive one or two strong inputs and sometimes a few additional weak inputs (Jaubert-Miazza et al., 2005; Hooks and Chen, 2006; Ziburkus and Guido, 2006). As expected for this age, we found that all WT cells were either refined or resolving (Figure 3.6C). However, we found no fully refined NP1/2 KO neurons at this age while many KO neurons remained unrefined (Figure 3.6C), which is consistent with the increased input number estimated above. Together these data indicate that NP1/2 KO dLGN neurons fail to prune their retinal inputs on a normal time course and suggest that collectively the excess inputs are capable of driving aberrantly large currents.

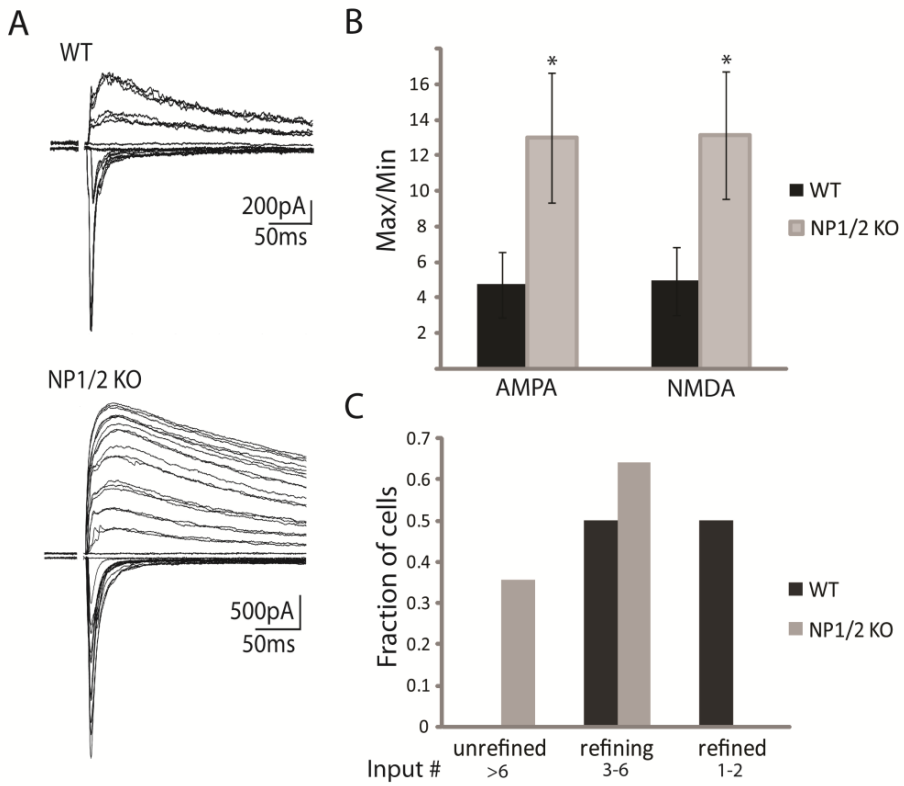

Figure 3.6 NP1/2 KOs display abnormal input elimination during development. (A) Example traces showing a [3] refined[4] P18 WT neuron (top) and an [3] unrefined[4] P18 NP1/2 KO neuron (bottom). **(B)** The total current divided by the presumably single fiber current for WT and NP1/2 KO neurons held at -70mV and +40mV. Dataset includes 17 WT cells from 6 animals and 17 KO cells from 7 animals. *p<0.05 **(C)** WT and KO neurons were classified into unrefined, resolving, and refined categories based on the number of stepwise increases in synaptic current amplitudes observed in response in increasing stimulus intensity. WT dataset includes 16 cells from 6 animals and KO dataset includes 14 cells from 6 animals.

Finally, the striking temporal correlation between the delayed development of AMPAR-mediated currents observed in this study and the delay in eye-specific segregation in the KOs that was previously reported begs the question of whether these processes might be linked. As a first step towards answering this question we sought to determine whether eye-specific segregation might be blocked at the level of retinogeniculate synapses in the NP1/2 KOs. Alternatively, as mentioned earlier NP1/2 KOs also displayed slightly altered retinal activity during this period. While none of the parameters of spontaneous RGC activity that are thought to be required for eye-specific segregation were altered in the NP1/2 KOs (Torborg et al., 2005; Bjartmar et al., 2006) it remains possible that increased spike frequency within bursts prevents eye-specific segregation in the KOs. To investigate the level of the circuit at which segregation is blocked in the absence of NP1/2 we employed *in vivo* drug administration and axon labeling. In WT animals, intraocular drug administration was previously used to show that eye-specific segregation is a competitive process (Penn et al., 1998; Stellwagen and Shatz, 2002). In these studies correlated retinal waves were either disrupted or enhanced in just one eye. The authors showed that reducing activity in one eye causes the axon arbors from the blocked eye to lose territory in the dLGN while the arbors from the untreated eye expand, and the converse is true when activity is enhanced in one eye. Here we used this protocol to determine the level of the circuit at which eye-specific segregation is blocked in the absence of NP1/2. If in the KOs retinal axons fail to refine because these animals experience slightly altered retinal activity, then pharmacological manipulations that dramatically perturb the balance of activity between the two eyes (for example, inhibiting activity in one eye) may be able to overcome this and drive axon remodeling in the KO dLGN. However, if in the NP1/2 KOs eye-specific segregation is blocked downstream of retinal activity (for instance, at the level of retinogeniculate synapses) then one would predict that axon refinement would remain blocked even when activity is reduced in one eye. For these experiments one eye was injected with epibatidine on P4, P6, and P8 to abolish correlated retinal waves and to reduce overall retinal spiking (Sun et al., 2008) between the ages of P4 and P10, the normal period for eye-specific segregation (Godement et al., 1984). The other eye was treated with saline.

Fluorescent dyes were injected into the eyes on P9 and brains were removed for analysis at P10. In addition, control groups of WT and KO animals received binocular saline injections. Our assumption in these experiments is that epibatidine blocks correlated retinal activity in KOs as well as in WTs, though we did not test this directly.

As was previously shown, we observed that in WT animals, epibatidine treatment led to a reduction in the size of the ipsilateral projection arising from the drug-treated eye and an expansion of the arbors from the saline-treated eye (Figure 3.7A,B, one-way ANOVA followed by Bonferroni's multiple comparisons test). In contrast to these WT findings, when performed on NP1/2 KO mice monocular injections of epibatidine failed to reduce the ipsilateral projection arising from the treated eye (Figure 3.7A,B). Animals treated with binocular saline injections showed no imbalance between the sizes of their ipsilateral projections regardless of genotype. These data indicate that when NP1/2 are absent axon remodeling in the dLGN is insensitive to manipulations of retinal activity, which strongly suggests that eye-specific segregation is blocked downstream of retinal activity in young NP1/2 KO mice. These data argue against altered retinal waves as being the primary cause of the abnormal eye-specific segregation in the NP1/2 KOs and are consistent with the idea that the loss of NP1/2 disrupts activity-dependent axon segregation at the level of the dLGN.

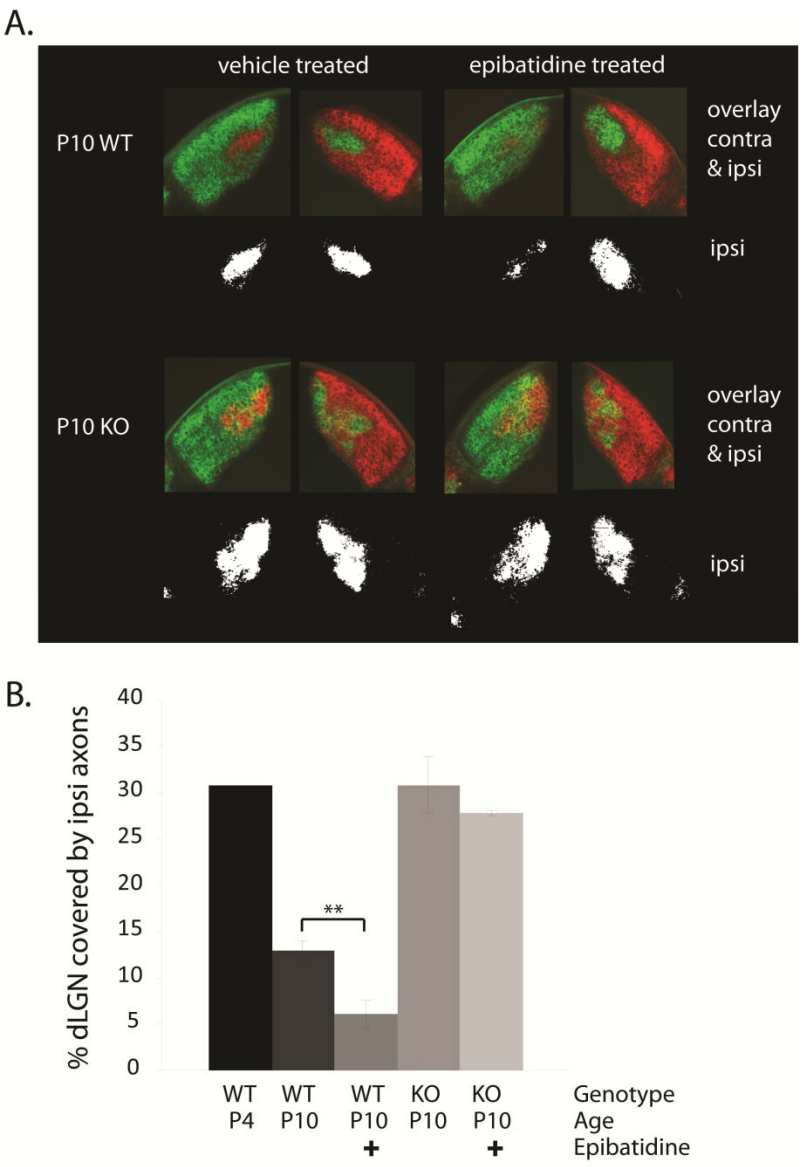

Figure 3.7 Monocular epibatidine treatment (P4-P10) fails to drive axon remodeling in NP1/2 KOs. **(A)** CTb-labeled RGC axons in vehicle-treated (left column) and epibatidine-treated (right column) WT animals (top row) and NP1/2 KOs (bottom row). Fluorescent images show both the contralateral and ipsilateral afferents. Black-and-white images display thresholded ipsilateral axons. Epibatidine-treated eye received red label. WT animal show diminished epibatidine treated ipsilateral projection. Epibatidine failed to diminish ipsilateral axons in NP1/2 KOs. **(B)** Percentage of dLGN area occupied by ipsilateral axons. In WT animals epibatidine treatment reduced ipsi-occupied area (n=3 WT vehicle-treated animals and n=4 WT drug-treated animals). Epibatidine had no effect on the ipsilateral axons in NP1/2 KO animals (n=4 KO animals per group). Ipsilateral projection is larger in the P10 KOs than in the WTs and is similar in size to the ipsi projection of an unrefined, P4 WT mouse. **(B,D)** Data displayed as mean+/-SEM. Comparison by one-way ANOVA and Bonferroni's multiple comparisons test *p<0.05.

3.3 Discussion

3.3.1 NP1/2 loss leads to reduced synaptic AMPAR-mediated currents in vivo

Here we report that in mice lacking NP1/2 AMPAR-mediated synaptic transmission is severely reduced in the visual thalamus during early postnatal life. This reduction can be explained by an increase in the number of synapses lacking detectable AMPAR-mediated currents with no accompanying changes in quantal size, paired pulse ratio, or NMDAR-mediated currents. These data are the first to demonstrate a requirement for NP1/2 in the establishment of AMPAR-mediated synaptic transmission *in vivo*.

Our finding that NPs are key factors mediating the early development of AMPAR-mediated transmission is well supported by previous studies of NP function in cell culture systems (O'Brien et al., 1999; O'Brien et al., 2002; Xu et al., 2003; Sia et al., 2007). However, that NP1/2 are specifically required for early silent synapse conversion is novel and not predicted from the earlier *in vitro* studies. For instance, Sia et al. recorded from HEK293T cells that were transfected with GluR4 and neuroligin and cultured on NP triple knockout hippocampal neurons and found a reduction in both the amplitude and frequency of their spontaneous currents (Sia et al., 2007). Similarly, based on biochemical and immunocytochemical data Xu et al. put forth a model in which NP1/2 modulate both the number and size of glutamate receptor clusters at excitatory synapses with NP1 stimulating modest increases in glutamate receptor aggregation over baseline and NP2 synergizing with NP1 to more dramatically increase this clustering (Xu et al., 2003). In contrast to these *in vitro* findings that suggest graded models of NP-dependent glutamate receptor recruitment, our *in situ* data is more consistent with a model in which NP1/2 are required for the synaptic localization of clusters of glutamate receptors in an all-or-none fashion.

Our results are also somewhat surprising given that AMPAR-mediated transmission was measured in NP1/2 KO hippocampal slices and was not found to be reduced (Bjartmar et al., 2006; Cho et al., 2008). There are at least three potential explanations for this discrepancy.

First, the mechanisms for AMPAR recruitment may vary across brain regions. Second, in this study we found that the requirement for NP1/2 was restricted to a specific developmental period, suggesting that deficits in hippocampal transmission may have been missed in the aforementioned studies since those recordings were performed at later ages. Finally, it has been suggested that NPs may act preferentially at excitatory synapses located on dendritic shafts (as opposed to spine synapses) (Mi et al., 2002). Since thalamic relay neurons are largely non-spiny (Rafols and Valverde, 1973; Kriebel, 1975) they receive nearly all of their excitatory input on dendritic shafts, and therefore, the loss of NP1/2 may more profoundly impact relay cell transmission (and that of other non-spiny neurons) than pyramidal cell transmission.

3.3.2 Are the affects of NP1/2 on retinogeniculate transmission direct?

NP1/2 are synaptic molecules that cluster AMPARs at synapses *in vitro*; therefore, it is reasonable to speculate that their loss from retinogeniculate synapses may alter AMPAR-mediated transmission. Alternatively, the effects of NP1/2 loss on retinogeniculate transmission could be an indirect consequence of alterations in upstream visual circuitry. Specifically, developing RGCs fire spontaneous bursts of action potentials and spike frequency during bursts was enhanced in the NP1/2 KOs. To begin to examine the affect of altered retinal spiking on retinogeniculate transmission we pharmacologically increased retinal spiking in WT animals *in vivo* over several days to determine if enhanced RGC spiking can reduce retinogeniculate transmission. Since increased retinal spiking had no affect on WT transmission this result argues against the idea that the enhanced spiking in the KOs is the major cause of their reduced AMPAR-mediated currents and is consistent with NP1/2 playing a direct role at developing retinogeniculate synapses. However, though cAMP treatment and NP1/2 loss both enhance retinal spiking their effects on retinal activity aren't identical; therefore, it remains possible that the specific aspects of retinal activity that are altered in the KOs may play a role in recruiting AMPARs to retinogeniculate synapses. An additional possibility is that the KO RGCs increase their spiking in an effort to compensate for their reduced ability to transmit signals to

their postsynaptic partners. In any case, NP1/2 are clearly required for the normal development of AMPAR-mediated currents at retinogeniculate synapses *in vivo*.

3.3.3 The requirement for NP1/2 is restricted to a specific developmental period

An important finding from this study is that the absence of NP1/2 leads to a deficit in silent synapse conversion during a specific developmental period, and that after P9 an NP1/2-independent mechanism arises which can compensate for the loss of NP1/2. This observation supports the emerging notion that nascent and more mature synapses employ different mechanisms for synaptic AMPAR recruitment. Studies have begun to demonstrate fundamental differences in the plasticity rules, signaling pathways, and expression mechanisms that govern synaptic AMPAR recruitment at immature and mature synapses. For example, immature and mature hippocampal synapses display different signaling pathways mediating long-term potentiation (Yasuda et al., 2003). The involvement of NMDAR activation in synaptic AMPAR expression also appears to change over development (Kim et al., 2005; Hall and Ghosh, 2008), and early and late synapses throughout the brain differ in a variety of molecular components including both NMDAR and AMPAR subunits (Zhu et al., 2000; Barria and Malinow, 2002; Ritter et al., 2002) as well as synaptic adhesion, signaling, and scaffolding molecules (Petralia et al., 2005). Though our results certainly do not exclude the possibility that NP1/2 may strengthen AMPAR-mediated transmission at more mature synapses, they strongly indicate that NP1/2 play an important role during the initial establishment of functional synaptic transmission and thereby contribute to our understanding of the mechanisms orchestrating the development of AMPAR-mediated transmission.

3.3.4 What is the basis of the excessive synaptic currents observed in the P17-P20 NP1/2 knockout animals?

We have previously reported that in the NP1/2 KO dLGN eye-specific segregation does not occur during the normal period for this process, but instead ensues later during the period that normally corresponds to within-eye segregation and functional input elimination (Bjartmar

et al., 2006). Here we show that in addition to delayed eye-specific segregation, functional input elimination is also altered in the absence of NP1/2. At P17 NP1/2 KO neurons received input from more RGCs than WT neurons at this age. This finding is likely to reflect a delay in input elimination rather than a permanent prevention of functional refinement since we observed some KO dLGN neurons that were clearly beginning to resolve, and from our previous study we know that eye-specific axons eventually sort themselves out in the KOs (Bjartmar et al., 2006). However, it remains possible that within-eye inputs may not completely segregate in the KOs.

Our finding that the extra RGC inputs were collectively capable of driving larger currents at retinogeniculate synapses is unique since other manipulations that have been shown to delay or prevent input elimination at this synapse do not appear to alter total current amplitudes. For instance, Hooks and Chen reported that retinal activity block with tetrototoxin between the ages examined here similarly prevents input elimination, but does not increase the total AMPAR or NMDAR-mediated currents (Hooks and Chen, 2006), and Stevens et al. found a similar phenotype in the absence of the classical immune molecule C1q (Stevens et al., 2007). These data suggest that excessive numbers of retinal inputs do not necessarily lead to excessive currents. In fact they suggest quite the opposite, that total current amplitude may be homeostatically regulated in dLGN neurons. This type of homeostasis has also been reported in the superior colliculus, another retino-recipient region (Shah and Crair, 2008b, a). In light of these previous findings, the enhanced synaptic currents observed in the older NP1/2 KO neurons may be due to the failure of such a homeostatic mechanism. For example, the early loss of AMPAR-mediated transmission in the NP1/2 KO mouse could lead to an elevation in the homeostatic set-point resulting in abnormally large AMPAR-mediated currents once these cells become capable of strengthening them. Interestingly, the AMPA/NMDA ratios of the older NP1/2 KO neurons were identical to their WT counterparts suggesting the amplitudes of the two current components may be mechanistically

linked. Whether NP1/2 play a role in homeostasis at this connection and what the nature of that role might be remain open questions for future studies.

In addition, it is worth noting that the third NP, NPR, has recently been shown to be required for mGluR1/5-dependent LTD in slices from P21-P29 hippocampus (Cho et al., 2008); therefore, an alternative explanation could be that while NP1/2 clearly strengthen AMPAR-mediated transmission early on, as development proceeds they may take on a new role in either limiting or weakening synaptic currents. However, it is unlikely that defective LTD can explain the excessive retinogeniculate currents observed in this study for two reasons: first, the Cho et al. study found no further deficit in LTD when NP1/2 were deleted in addition to NPR, and second, retinogeniculate synapses are not thought to express mGluRs (Godwin et al., 1996; Salt, 2002).

Finally, if NP1/2 play a role in the generation of stage III (glutamatergic) retinal waves then the KOs may experience abnormal retinal activity during within eye segregation, which could contribute to their altered input elimination during this period. The basis of the excessive synaptic currents and the role of NP1/2 during within eye segregation will be interesting topics for additional studies.

3.3.5 What mechanisms underlie the eye-specific segregation defect in the NP1/2 KOs?

In our previous study we demonstrated that in the NP1/2 KO mouse retinal axons fail to undergo eye-specific refinement during the normal period for this process; however, the mechanistic basis of this anatomical defect remained unclear (Bjartmar et al., 2006). Eye-specific segregation requires spontaneous spiking activity in the retina (Shatz and Stryker, 1988; Sretavan et al., 1988), and the structure of the this activity is thought to instruct synaptic competition in the dLGN (Penn et al., 1998; Rossi et al., 2001; Muir-Robinson et al., 2002; Stellwagen and Shatz, 2002; Stafford et al., 2009; but see Huberman et al., 2003). Like WT RGCs, NP1/2 KO RGCs fired periodic bursts of action potentials and KO retinas displayed propagating waves of retinal activity during eye-specific segregation. In addition many of the

features of retinal waves that are thought to be important for driving segregation were intact in the KOs (KO RGCs fired action potentials within high-frequency bursts, bursting among neighboring KO RGCs was highly correlated, correlated firing diminished with distance, and inter-burst intervals were identical between WTs and KOs). Despite this, some differences between WT and KO waves were apparent and could contribute to the delayed segregation (Bjartmar et al., 2006). Namely, NP1/2 KO RGCs exhibited increased spike frequencies during bursts which resulted in both neighboring and more distant KO RGCs firing greater numbers of synchronous spikes. Consequently, we performed an experiment to begin to investigate the impact of altered retinal activity on eye-specific segregation in the NP1/2 KOs. Retinal waves were pharmacologically blocked in one eye over the period of eye-specific segregation using epibatidine (our presumption is that epibatidine also blocks waves in the KO retinas). Similar to previous reports, we found that in WT animals monocular blockade of retinal activity caused the axons from the drug-treated eye to lose territory in the dLGN while the axons from the saline-treated eye expanded; however, in the absence of NP1/2 monocular activity blockade had no effect on the arborization patterns of RGC axons. The insensitivity of NP1/2 KO axons to the manipulation of retinal activity suggests that eye-specific refinement may be blocked downstream of retinal activity when NP1/2 are absent, perhaps at the level of retinogeniculate synapses. Thus, NP1/2 may be among a small number of molecules currently shown to sit at the crossroads between structural and functional plasticity in this developing circuit (Upton et al., 1999; Huh et al., 2000; Menna et al., 2003; Stevens et al., 2007). However, additional experiments will clearly be required to clarify the relationships between the functional and structural phenotypes in the NP1/2 KO mouse.

In summary, the findings presented here demonstrate that NP1/2 are required *in vivo* for the normal development of AMPAR-mediated synaptic transmission and specifically implicate NP1/2 in silent synapse conversion. These data provide new insight into the molecular mechanisms for AMPAR recruitment at nascent versus mature synapses. In addition, the requirement for NP1/2 was restricted to an early developmental period when neural

circuits are undergoing dramatic remodeling suggesting that NP1/2-dependent synaptic strengthening could contribute to developmental circuit refinement.

3.4 *Materials and Methods*

Animals.

All experiments were performed in accordance with the animal handling guidelines put forward by the Institutional Animal Care and Use Committee. The generation of the NP1/2 KO animals has been previously described (Kirkpatrick et al., 2000; Bjartmar et al., 2006).

Slice preparation.

NP1/2 double knockout mice were bred to C57BL/6 background for 7 generations to make congenic NP1/2 C57BL/6 mice. Acute slices (325μm) were prepared from WT C57BL/6 mice or from mice that were either knockouts or heterozygous for NP1 and NP2 using the method of Chen and Regehr, which preserves the optic tract and dLGN (Chen and Regehr, 2000). Throughout the course of the experiments two different cutting solutions were used; either a high-sucrose based solution containing (in mM): 50.0 NaCl, 25.0 $NaHCO_3$, 150.0 Sucrose, 10.0 Dextrose, 2.5 KCl, 1.0 NaH_2PO_4, 0.5 $CaCl_2$, 7.0 $MgCl_2*6H_20$, or a choline-based solution containing (in mM): 78.3 NaCl, 23.0 $NaHCO_3$, 23.0 Dextrose, 33.8 Choline Chloride, 2.3 KCl, 1.1 NaH_2PO_4, 6.4 $MgCl_2$, 0.45 $CaCl_2$. Chemicals were obtained from Sigma. After cutting, slices were incubated in oxygenated, 32-34°C cutting solution for 25-40 minutes and then transferred to oxygenated ACSF consisting of (in mM): 125.0 NaCl, 25.0 $NaHCO_3$, 25.0 Dextrose, 2.5 KCl, 1.25 NaH_2PO_4, 2.0 $CaCl_2$, 1.0 $MgCl_2*6H_20$. For recordings of quantal events calcium was omitted from the recording solution and replaced with 3mM strontium. Slices were incubated in ACSF for 25-40 minutes during which time they were allowed to cool to room temperature. Slices were continuously perfused with oxygenated ACSF during the recording period.

Electrophysiology

Whole-cell voltage-clamp recordings of geniculate neurons were obtained using 2.5-3.5MOhm patch electrodes containing an internal solution consisting of (in mM): 35 CsF, 100

CsCl, 10 EGTA, and 10 HEPES. Inhibitory inputs were blocked with 20μM bicuculline methobromide (Tocris). Recordings were sampled at 10-20kHz and filtered at 1kHz. Access resistance was monitored throughout the recording period and was adjusted to 4-9MOhms after 70% compensation. A stimulating electrode (either concentric bipolar or two glass electrodes filled with ACSF) was placed just touching the surface of the optic tract next to the ventral LGN, and 1msec stimuli ranging from 0 to 40μA were delivered every 30-60 seconds. NMDAR-mediated current amplitudes were measured at a holding potential of +40mV by evoking synaptic currents and measuring the peak of the current trace at a time when the AMPAR-mediated currents no longer contributed to the response: 20-30ms after the onset of the EPSC for the P6-P9 recordings, and 10-15ms after EPSC onset for the P17-P20 recordings. Synaptic currents were analyzed using a variety of software programs including Igor Pro, Synaptosoft Mini Analysis, Microsoft Excel, and GraphPad Prism. Statistical comparisons were made using a Student's unpaired t-test unless otherwise stated.

Intraocular injections

Mice were anesthetized with isoflurane and fused eyelids were gently separated with tweezers. A 30.5 gauge beveled syringe tip was used to pierce the eye at the corneal-scleral junction. This allowed some vitreal solution to escape, releasing some of the intraocular pressure. After the escaped vitreous was wicked away a blunt-tipped Hamilton syringe was inserted into the hole and 0.5-1.0μL of solution was injected (0.5 μL for P4 mice, 0.75 μL for P6 mice, and 1.0 μL for P8/9). To increase retinal activity a 2mM solution of CPT-cAMP (Tocris) was injected binocularly. For experiments in which spontaneous activity was blocked in one eye a 1mM solution of epibatidine (Sigma) was injected into the right eye and a saline-only solution was injected into the left eye. For anterograde labeling of RGC axons a 0.5% solution (in saline) of the ß subunit of choleratoxin conjugated to Alexa 594 (Molecular Probes) was injected into the epibatidine-treated eye and an Alexa 488 conjugate was injected into the control-treated eye. Control animals received binocular saline injections followed by Ctß-594 and Ctß-488 in the right and left eyes, respectively.

Analysis of retinogeniculate projections

Brains were removed 24 hours after intraocular injection with the fluorescent tracers and fixed overnight in 4.0% PFA. 50μM coronal sections were prepared using a Leica vibrating microtome and imaged on a Nikon Eclipse microscope. Images were taken using a Photometrics Coolsnap camera and imported into Adobe Photoshop for analysis. Grayscale images were converted into binary (black and white) images using a threshold that corresponded to a location in the grayscale histogram where there was a clear distinction between the label and background fluorescence signals, values typically corresponded ~30 on the grayscale range of 0-255 (Muir-Robinson et al., 2002; Torborg and Feller, 2004). Thresholded images were imported into ImageJ. The boundaries of the dLGN were delineated in order to exclude label from the optic tract, intrageniculae leaflet, and ventral LGN. Measurements of the area of the dLGN occupied by the ipsilateral projections were calculated by selecting all white pixels within the delineated area.

Chapter 4 — Discussion

4.1 What is the role of glutamatergic synaptic transmission in eye-specific refinement?

What do the findings from VGluT2 reduction and NP1/2 knockout tell us about the role of glutamatergic transmission in eye-specific visual circuit refinement? A commonality between the two studies is that in both cases glutamatergic synaptic transmission was reduced at RGC-dLGN synapses during eye-specific refinement and in both cases eye-specific refinement failed. The major differences between the studies are that NP1/2 KO specifically reduced AMPAR-mediated synaptic transmission at all synapses, whereas VGluT2 reduction reduced both AMPAR-mediated and NMDAR-mediated synaptic transmission equally and only in ipsilateral-projecting RGCs. Together, the findings from the two studies strongly suggest that glutamatergic transmission plays an important role in translating retinal activity patterns into altered axonal projection patterns. Furthermore, the restriction of VGluT2 reduction to ipsilateral-projecting RGCs can explain why only select features of eye-specific refinement were altered in that study (Figures 2.6-2.9), while NP1/2 loss impacted eye-specific refinement more broadly (Bjartmar et al., 2006). One caveat of these findings is that in neither study was glutamatergic transmission eliminated; therefore we are unable to conclude whether glutamate release or AMPAR-mediated transmission is required for axonal refinement. In both studies we observed some animals that exhibited no glutamate release or no AMPAR currents; thus, considering that eye-specific refinement was abnormal in all VGluT2-deficient and NP1/2 KO animals, this suggests that glutamatergic synaptic transmission is probably required.

Our finding that contra-RGC axons persist in the ipsi-eye territory when ipsi axons are deficient in VGluT2, strongly suggests that glutamate release plays a specific and important role in ejecting axons from inappropriate target regions during visual circuit refinement. If this is the case then we would predict that blocking glutamatergic transmission in all RGCs would prevent both ipsi and contra axons from consolidating into their normal eye-specific territories. This prediction is supported by our NP1/2 KO findings, in which AMPAR currents were reduced at all RGC-dLGN synapses and both ipsi and contra-eye axons failed to refine (Figure 3.1 and

Bjartmar et al., 2006). One caveat with that interpretation, however, is that it is still not clear why eye-specific segregation fails in NP1/2 KO mice since those mice also exhibited altered retinal waves. Thus, additional studies are required to determine the exact role(s) played by NP1/2 in RGC axon refinement. In the future, we may be able to test our prediction more directly by removing VGluT2 from all (or most) RGCs by crossing the conditional VGluT2 knockouts to a pan-RGC Cre line. Regardless, our present VGluT2 findings alone strongly suggest that glutamate-based competition drives competing-RGC axons out of the ipsi-eye territory.

4.2 What is the glutamate-dependent mechanism that eliminates mis-targeted axons?

Our neuronal pentraxin findings suggest that postsynaptic AMPAR currents may contribute to the competitive mechanism by which ipsi-RGC axons drive contra-RGC axons out of their territory. Could activation of AMPARs at ipsilateral synapses exert heterosynaptic effects on neighboring contralateral synapses? The dendrites of dLGN neurons do not contain spines; consequently, synaptic inputs are probably not well isolated from each other. This suggests that postynaptic membrane depolarization and calcium influxes (through NMDARs or L-type calcium channels) could travel some distance along the dendritic shaft. In this scenario intracellular calcium concentrations would likely be higher at the initial synaptic contact than at neighboring synapses, which could differentially affect their plasticity and stability (Chistiakova and Volgushev, 2009). Glutamate spillover is another mechanism that could inhibit adjacent synapses through receptor desensitization (Voronin and Cherubini, 2004). Another potential contributing factor could be differential expression of synaptic components that alter synaptic transmission at ipsilateral versus contralateral synapses. Two examples of synaptic components that are selectively found in ipsilateral axons include synaptically-localized zinc (Land and Shamalla-Hannah, 2001) and the serotonin transporter, SERT (Lebrand et al., 1996; Upton et al., 1999).

Zinc can be packaged in synaptic vesicles by the neuronal zinc transporter, ZnT-3, and released from synapses in response to neural activity (see Paoletti et al., 2009 for a review of

zinc action at glutamate synapses). Released zinc can potentiate AMPARs and inhibit glutamate transporters, which could selectively enhance glutamatergic currents at ipsilateral synapses. Zinc also inhibits NMDARs, which could specifically inhibit ipsilateral transmission and plasticity. On the other hand, zinc spillover has been hypothesized to play a role in heterosynaptic inhibition since zinc may diffuse a fair distance and NMDARs are inhibited at even low concentrations of zinc (Ueno et al., 2002). Another possibility is that zinc is selectively sequestered into ipsilateral terminals as a protective mechanism to prevent inhibition of their NMDARs. Though it is not straight forward to predict how zinc localization affects ipsilateral synapases and axons, the selective localization of zinc to ipsilateral terminals is intriguing. ZnT-3 knockout animals exist and it would be interesting to see if they have eye-specific segregation deficits (Cole et al., 1999).

SERT is also specifically expressed by ipsi-RGCs and SERT removal blocks eye-specific refinement (Lebrand et al., 1996; Upton et al., 1999; Upton et al., 2002). In the Upton et al. studies SERT loss led to overlapping contra and ipsi axons primarily through a failure of contra axons to evacuate the ipsi territory -the same phenotype that we found with VGluT2 reduction in ipsi-RGCs. RGCs also transiently express the vesicular monoamine transpoter 2 (VMAT2) and the $5HT_{1B}$ receptor during development. Selective SERT expression in ipsi-RGCs could allow them to 1) uptake serotonin using SERT and package it into vesicles for release (using VMAT2), or to 2) remove serotonin from the synaptic cleft using SERT in order to reduce serotonin occupation of their $5HT_{1B}$ receptors. Since presynaptic serotonin receptors often inhibit neurotransmitter release, selective SERT expression in ipsi-RGC axons might give ipsi-RGC axons a competitive advantage by protecting them from serotonin-mediated inhibition of glutamate release. In support of the second hypothesis, $5HT_{1B}$ removal rescued the eye-specific segregation defect in SERT KOs. Differential effects of serotonin on contralateral versus ipsilateral synaptic transmission could be tested by selectively stimulating either ipsilateral or contralateral axons and recording postsynaptic currents in the presence and absence of serotonin. In addition to SERT and zinc, other synaptic components may also be

differentially localized to ipsi versus contra axons. With an ipsi-RGC specific Cre line in hand, it should now be possible to sort ipsi and contra RGCs and to fully characterize the genes that are differentially expressed between the two populations over development.

In addition to the loss of effective ipsilateral competition that results from VGluT2 reduction in ipsi-RGCs, homeostatic mechanisms may also contribute to the persistence of the contra-RGC axons in the ipsi-eye territory. For instance, dLGN neurons have been reported to homeostatically regulate their total synaptic drive (Chandrasekaran et al., 2007; Hooks and Chen, 2006; Shah and Crair, 2008; Stevens et al., 2007), so when ipsi-RGC inputs are weakened (by VGluT2 reduction) homeostatic mechanisms might play a role in maintaining and strengthening contra-RGC inputs that would normally be eliminated. It would be interesting to measure total response sizes of dLGN neurons in the ipsi-eye territory in ET33-Cre::VGluT2$^{flox/flox}$ animals to see if they are precisely targeted to wild type levels.

4.3 Does glutamatergic synaptic transmission stabilize developing RGC axons?

While our experiments clearly demonstrate a role for glutamate in eliminating mis-targeted axons during visual circuit refinement, the role of glutamate in stabilizing appropriately targeted axons is less clear. Studies of RGC axons in the frog optic tectum suggest that activity stimulates BDNF release which is essential for stabilizing RGC synapses and axons (Hu et al., 2005; Marshak et al., 2007). However, a mouse knockout study showed that Trk-B is not required for eye-specific refinement (Rodger and Frost, 2009), and removal of Trk-B from ipsi-RGCs does not prevent the establishment or maintenance of the ipsi-eye territory or eye-specific segregation (unpublished data from the Ullian lab). Still, a low level of glutamate release may be required to stabilize individual RGC axons and synapses either through neurotrophic support or another mechanism. Morphological assessment of single VGluT2-deficient ipsi-RGC axons and their synapses could help to determine whether cellular abnormalities arise when glutamate release is reduced. In any case, our findings suggest that the mechanism that eliminates axons from inappropriate target regions is considerably more sensitive to manipulations of synaptic glutamate than the mechanism that stabilizes

appropriately targeted axons. Thus, the stabilization of appropriate circuit connections and the elimination of inappropriate connections are separable by their differential sensitivities to glutamate levels.

4.4 Summary

By removing neuronal pentraxins 1 and 2 we were able to show that these proteins play a specific role in establishing AMPAR-mediated synaptic currents at RGC-dLGN synapses. Those findings are significant because, to date, little is known about the synaptic molecules that mediate retinogeniculate synaptic development and refinement and because they were the first demonstration that NP1/2 are required in vivo for the normal development of AMPAR-synaptic transmission. In addition, by reducing VGluT2 selectively in ipsilateral-projecting RGCs we were able to show that glutamate release mediates competition among axonal inputs within developing CNS circuits. Therefore, the experiments in this dissertation shed new light on the development of AMPAR-mediated synaptic transmission at RGC-dLGN synapses and on the direct contributions of glutamate to the refinement of visual circuitry.

References

Barria A, Malinow R (2002) Subunit-specific NMDA receptor trafficking to synapses. Neuron 35:345-353.

Bansal A, Singer JH, Hwang BJ, Xu W, Beaudet A, Feller MB (2000) Mice lacking specific nicotinic acetylcholine receptor subunites exhibit dramatically altred spontaneous activity patterns and reveal a limited role for retinal waves in forming ON and OFF circuits in the inner retina. J Neurosci 20:7672-7681.

Bickford ME, Slusarczyk A, Dilger EK, Krahe TE, Kucuk C, Guido W (2010) Synaptic development of the mouse dorsal lateral geniculate nucleus. J Comp Neurol 518:622-625.

Bjartmar L, Huberman AD, Ullian EM, Renteria RC, Liu X, Xu W, Prezioso J, Susman MW, Stellwagen D, Stokes CC, Cho R, Worley P, Malenka RC, Ball S, Peachey NS, Copenhagen D, Chapman B, Nakamoto M, Barres BA, Perin MS (2006) Neuronal pentraxins mediate synaptic refinement in the developing visual system. J Neurosci 26:6269-6281.

Butts DA, Kanold PO, Shatz CJ (2007) A burst-based "Hebbian" learning rule at retinogeniculate synapses links retinal waves to activity-dependent refinement. PLoS Biol 5,e61.

Chapmen B (2000) Necessity for afferent activity to maintain eye-specific segregation in ferret lateral geniculate nucleus. Science 287: 2479-2482.

Chen C, Regehr WG (2000) Developmental remodeling of the retinogeniculate synapse. Neuron 28:955-966.

Chen C, Regehr WG (2003) Presynaptic modulation of the retinogeniculate synapse. J Neurosci 23:3130-3135.

Chistiakova M, Volgushev M (2009) Heterosynaptic plasticity in the neocortex. Exp Brain Res 199:377-390.

Cho RW, Park JM, Wolff SB, Xu D, Hopf C, Kim JA, Reddy RC, Petralia RS, Perin MS, Linden DJ, Worley PF (2008) mGluR1/5-dependent long-term depression requires the regulated ectodomain cleavage of neuronal pentraxin NPR by TACE. Neuron 57:858-871.

Cole TB, Wenzel HJ, Kafer KE, Schwartzkroin PA, Palmiter RD (1999) Elimination of zinc from synaptic vesicles in the intact mouse brain by disruption of the ZnT3 gene. Proc natl Acad Sci USA 96;1716-21.

Cook PM, Prusy G, Ramoa AS (1999) The role of spontaneous retinal activity before eye opening in the maturation of form and function in the retinogeniculate pathway of the ferret. Vis Neurosci 16:491-501.

Crair MC, Gillespia DC, Stryker MP (1998) The role of visual experience in the development of columns in cat visual cortex. Science 279:566-570.

Crair MC, Horton JC, Antoninin A, Stryker MP (2001) Emergence of ocular dominance columns in cat visual cortex by 2 weeks of age. J Comp Neurol 430:235-249.

Demas J, Sagdullaev BT, Green E, Jaubert-Miazza L, MacCall MA, Gregg RG, Wong RO, Guido W (2006) Failure to maintain eye-specific segregation in nob, a mutant with abnormally patterned retinal activity. Neuron 50:247-259.

Drager UC, Olsen JF (1980) Origins of crossed and uncrossed retinal projections in pigmented and albino mice. J Comp Neurol 191:383-412.

Fujiyama F, Hioki H, Tomioka R, Taki K, Tamamaki N, Nomura S, Okamoto K, Kaneko T (2003) Changes of immunocytochemical localization of vesicular glutamate transporters in the rat visual system after the retinofugal denervation. J Comp Neurol 465:234-249.

Garcia-Frigola C, Herrera E (2010) Zic2 regulates the expression of Sert to modulate eye-specific refinement at the visual targets. EMBO J 29:3170-3183.

Godement P, Salaun J, Imbert M (1984) Prenatal and postnatal development of retinogeniculate and retinocollicular projections in the mouse. J Comp Neurol 230:552-575.

Godwin DW, Van Horn SC, Eriir A, Sesma M, Romano C, Sherman SM (1996) Ultrastructural localization suggests that retinal and cortical inputs access different metabotropic glutamate receptors in the lateral geniculate nucleus. J Neurosci 16:8181-8192.

Gong S, Doughty M, Harbaugh CR, Cummins A, Hatten ME, Heintz N, Gerfen CR (2007) Targeting Cre recombinase to specific neuron populations with bacterial artificial chrommosome constructs. J Neurosci 27:9817-9823.

Hall BJ, Ghosh A (2008) Regulation of AMPA receptor recruitment at developing synapses. Trends Neurosci 31:82-89.

Herrera E, Brown L, Aruga J, Rachel RA, Dolen G, Mikoshiba K Brown S, Mason C (2003) Zic2 patterns binocular vision by specifying the uncrossed retinal projection. Cell 114:;545-557.

Hippenmeyer S, Vrieseling E, Sigrist M, Portmann T, Laengle C, Ladle DR, Arber S (2005) A developmental switch in the response of DRG neurons to ETS transcription factor signaling. PloS Biol 3,e159.

Hooks BM, Chen C (2006) Distinct roles for spontaneous and visual activity in remodeling of the retinogeniculate synapse. Neuron 52:281-291.

Hnasko TS, Chuhma N, Zhang H, Goh GY, Sulzer D, Palmiter RD, Rayport S, Edwards RH (2010) Vesicular glutamate transport promotes dopamine storage and glutamate corelease in vivo. Neuron 65:643-656.

Hu B, Nikoakopoulou AM, Cohen-Corey S (2005) BDNF stabilizes synapses and maintains the structural complexity of optic axon in vivo. Development 132:4285-98.

Huberman AD, Feller MB, Chapman B (2008a) Mechanisms underlying development of visual maps and receptive fields. Annu Rev Neurosci 31:479-509.

Huberman AD, Manu M, Koch SM, Susman MW, Lutz AB, Ullian EM, Baccus SA, Barres BA (2008b) Architecture and activity-mediated refinement of axonal projections from a mosaic of genetically identified retinal ganglion cells. Neuron 59:425-438.

Huberman AD, Wang GY, Liets LC, Collins OA, Chapman B, Chalupa LM (2003) Eye-specific retinogeniculate segregation independent of normal neuronal activity. Science 300:994-998.

Huh GS, Boulanger LM, Du H, Riquelme PA, Brotz TM, Shatz CJ (2000) Functional requirement for class I MHC in CNS development and plasticity. Science 290:2155-2159.

Jaubert-Miazza L, Green E, Lo FS, Bui K, Mills J, Guido W (2005) Structural and functional composition of the developing retinogeniculate pathway in the mouse. Vis Neurosci 22:661-676.

Johnson H, Tian N, Caywood MS, Reimer RJ, Edwards RH, Copenhagen DR (2003) Vesicular neurotransmitter transporter expression in developing postnatal rodent retina: GABA and glycine precede glutamate. J Neurosci 23:518-529.

Katz LC, Shatz CJ (1996) Synaptic activity and the construction of cortical circuits. Science 275:1133-1138.

Kim MJ, Dunah AW, Wang YT, Sheng M (2005) Differential roles of NR2A- and NR2B-containing NMDA receptors in Ras-ERK signaling and AMPA receptor trafficking. Neuron 46:745-760.

Kirkpatrick LL, Matzuk MM, Dodds DC, Perin MS (2000) Biochemical interactions of the neuronal pentraxins. Neuronal pentraxin (NP) receptor binds to taipoxin and taipoxin-associated calcium-binding protein 49 via NP1 and NP2. J Biol Chem 275:17786-17792.

Koch SM, Ullian EM (2010) Neuronal pentraxins mediate silent synapse conversion in the developing visual system. J Neurosci 31:5405-5414.

Kriebel RM (1975) Neurons of the dorsal lateral geniculate nucleus of the albino rat. J Comp Neurol 159:45-67.

Land PW, Shamalla-HannahL (2001) Transient expression of synaptic zinc during development of uncrossed retinogeniculate projections. J Comp Neurol 422:515-25.

Lebrand C, Cases O, Adelbrecht D, Doye A, Alvarez C, El Mestikawy D, Seif I. Gaspar P (1996). Transient uptake and storage of serotonin in developing thalamic neurons. Neuron 17:823-835.

Liu X, Chen C (2008) Different roles for AMPA and NMDA receptors in transmission at the immature retinogeniculate synapse. J Neurophysiol 99:629-643.

Madisen L, Zwingman TA, Sunkin SM, Oh SW, Zuriwala HA, Gu H NG LL, Palmiter RD, Hawrylycz MJ, Jones AR, Lein ES, Zeng H (2009) A robust and high-throughput Cre reporting and characterization system for the whole mouse brain. Nat Neurosci 13:133-142.

Marshak S, Nikolakopoulou AM, Dirks R, Martens GJ, Cohen-Cory S (2007) J Neurosci. 27:2444-56.

Menna E, Cenni MC, Naska S, Maffei L (2003) The anterogradely transported BDNF promotes retinal axon remodeling during eye specific segregation within the LGN. Mol Cell Neurosci 24:972-983.

Meyer-Franke A, Kaplan MR, Pfieger FW, Barres BA (1995) Characterization of the signaling interactions that promote the survival and growth of developing retinal ganglion cells in culture. Neuron 15:805-819.

Mi R, Tang X, Sutter R, Xu D, Worley P, O'Brien RJ (2002) Differing mechanisms for glutamate receptor aggregation on dendritic spines and shafts in cultured hippocampal neurons. J Neurosci 22:7606-7616.

Miledi R (1966) Strontium as a substitute for calcium in the process of transmitter release at the neuromuscular junction. Nature 212:2.

Muir-Robinson G, Hwang BJ, Feller MB (2002) Retinogeniculate axons undergo eye-specific segregation in the absence of eye-specific layers. J Neurosci 22:5259-5264.

Narboux-Neme N, Pavone LM, Avallone L, Zhuang X, Gaspar P (2008) Serotonin transporter transgenic (SERTcre) mouse line reveals developmental targets of serotonin specific reuptake inhibitors (SSRIs). Neuropharmacology 55:994-1005.

O'Brien R, Xu D, Mi R, Tang X, Hopf C, Worley P (2002) Synaptically targeted narp plays an essential role in the aggregation of AMPA receptors at excitatory synapses in cultured spinal neurons. J Neurosci 22:4487-4498.

O'Brien RJ, Xu D, Petralia RS, Steward O, Huganir RL, Worley P (1999) Synaptic clustering of AMPA receptors by the extracellular immediate-early gene product Narp. Neuron 23:309-323.

Penn AA, Riquelme PA, Feller MB, Shatz CJ (1998) Competition in retinogeniculate patterning driven by spontaneous activity. Science 279:2108-2112.

Petralia RS, Sans N, Wang YX, Wenthold RJ (2005) Ontogeny of postsynaptic density proteins at glutamatergic synapses. Mol Cell Neurosci 29:436-452.

Rafols JA, Valverde F (1973) The structure of the dorsal lateral geniculate nucleus in the mouse. A Golgi and electron microscopic study. J Comp Neurol 150:303-332.

Rebsam A, Petros TJ, Mason CA (2009) Switching retinogeniculate axon laterality leads to normal targeting but abnormal eye-specific segregation that is activity-dependent. J Neurosci 29:14855-63.

Reti IM, Reddy R, Worley PF, Baraban JM (2002) Prominent Narp expression in projection pathways and terminal fields. J Neurochem 82:935-944.

Ritter LM, Vazquez DM, Meador-Woodruff JH (2002) Ontogeny of ionotropic glutamate receptor subunit expression in the rat hippocampus. Brain Res Dev Brain Res 139:227-236.

Rodger J and Frost DO (2009) Effects of trkB knockout on topography and ocular segregation of uncrossed retinal projections. Exp Brain Res 195:35-44.

Rossi FM, Pizzorusso T, Porciatti V, Marubio LM, Maffei L, Changeux JP (2001) Requirement of the nicotinic acetylcholine receptor beta 2 subunit for the anatomical and functional development of the visual system. Proc Natl Acad Sci U S A 98:6453-6458.

Sanes JR, Lichtman JW, (1999) Development of the vertebrate neuromuscular junction. Annu Rev Neurosci 22:289-442.

Salt TE (2002) Glutamate receptor functions in sensory relay in the thalamus. Philos Trans R Soc Lond B Biol Sci 357:1759-1766.

Shah RD, Crair MC (2008a) Retinocollicular synapse maturation and plasticity are regulated by correlated retinal waves. J Neurosci 28:292-303.

Shah RD, Crair MC (2008b) Mechanisms of response homeostasis during retinocollicular map formation. J Physiol 586:4363-4369.

Shatz CJ, Sretavan DW (1986) Interactions between retinal ganglion cells during the development of the mammalian visual system. Annu Rev Neurosci 9:171-207.

Shatz CJ, Stryker MP (1988) Prenatal tetrodotoxin infusion blocks segregation of retinogeniculate afferents. Science 242:87-89.

Sherry DM, Wang MM, Bates J, Freshman LJ (2003) Expression of vesicular glutamate transporter 1 in the mouse retina reveals temporal ordering in development of rod vs. cone and ON vs OFF circuits. J Comp Neurol 465:480-498.

Sia GM, Beique JC, Rumbaugh G, Cho R, Worley PF, Huganir RL (2007) Interaction of the N-Terminal Domain of the AMPA Receptor GluR4 Subunit with the Neuronal Pentraxin NP1 Mediates GluR4 Synaptic Recruitment. Neuron 55:87-102.

Soriano P (1999) Generalized lacZ expression with the ROSA26 Cre reporter strain. Nat Genet 21: 70-71.

Sretavan DW, Shatz CJ, Stryker MP (1988) Modification of retinal ganglion cell axon morphology by prenatal infusion of tetrodotoxin. Nature 336:468-471.

Stafford BK, Sher A, Litke AM, Feldheim DA (2009) Spatial-temporal patterns of retinal waves underlying activity-dependent refinement of retinofugal projections. Neuron 64:200-212.

Stella SL, Jr Li S, Sabatini A, Vila A, Brecha NC (2008) Comparison of the ontogeny of the vesicular glutamate transporter 3 (VGLUT3) with VGLUT1 and VGLUT2 in the retina. Brain Res 1215:20-29.

Stellwagen D, Shatz CJ (2002) An instructive role for retinal waves in the development of retinogeniculate connectivity. Neuron 33:357-367.

Stellwagen D, Shatz CJ, Feller MB (1999) Dynamics of retinal waves are controlled by cyclic AMP. Neuron 24:673-685.

Stevens B, Allen NJ, Vazquez LE, Howell GR, Christopherson KS, Nouri N, Micheva KD, Mehalow AK, Huberman AD, Stafford B, Sher A, Litke AM, Lambris JD, Smith SJ, John SW, Barres BA (2007) The classical complement cascade mediates CNS synapse elimination. Cell 131:1164-1178.

Stuber GD, Hnasko TS, Britt JP, Edwards RH, Bonci A (2010) Dopamineric terminals in the nucleus accumbens but not the dorsal striatum corelease glutamate. J Neurosci 30:8229-8233.

Sun C, Speer CM, Wang GY, Chapman B, Chalupa LM (2008) Epibatidine application in vitro blocks retinal waves without silencing all retinal ganglion cell action potentials in developing retina of the mouse and ferret. J Neurophysiol 100:3253-3263.

Torborg CL, Feller MB (2004) Unbiased analysis of bulk axonal segregation patterns. J Neurosci Methods 135:17-26.

Torborg CL, Hansen KA, Feller MB (2005) High frequency, synchronized bursting drives eye-specific segregation of retinogeniculate projections. Nat Neurosci 8:72-78.

Upton AL, Salichon N, Lebrand C, Ravary A, Blakely R, Seif I, Gaspar P (1999) Excess of serotonin (5-HT) alters the segregation of ispilateral and contralateral retinal projections in monoamine oxidase A knock-out mice: possible role of 5-HT uptake in retinal ganglion cells during development. J Neurosci 19:7007-7024.

Upton AL, Ravary A, Salichon N, Moessner R, Lesch KP, Hen R, Seif I, Gaspar P (2002) Lack of 5-HT_{1B} receptor and of serotonin transporter have different effects on the segregation of retinal axon in the lateral genicualte nucleus compared to the superior colliculus. Neuroscience 111:397-610.

Voronin LL, Cherubini E (2004) 'Deaf, mute and whispering' silent synapses: their role in synaptic plasticity. J Physiol 557:3-12.

Xiao MY, Wasling P, Hanse E, Gustafsson B (2004) Creation of AMPA-silent synapses in the neonatal hippocampus. Nat Neurosci 7:236-243.

Xu D, Hopf C, Reddy R, Cho RW, Guo L, Lanahan A, Petralia RS, Wenthold RJ, O'Brien RJ, Worley P (2003) Narp and NP1 form heterocomplexes that function in developmental and activity-dependent synaptic plasticity. Neuron 39:513-528.

Xu HP, Chen H, Ding Q, Xie ZH, Chen L, Diao L, Wang P, Gan L, Crair MC, Tian N (2010) The immune protein CD3zeta is required for normal development of neural circuits in the retina. Neuron 65:5-3-15.

Yasuda H, Barth AL, Stellwagen D, Malenka RC (2003) A developmental switch in the signaling cascades for LTP induction. Nat Neurosci 6:15-16.

Zhu JJ, Esteban JA, Hayashi Y, Malinow R (2000) Postnatal synaptic potentiation: delivery of GluR4-containing AMPA receptors by spontaneous activity. Nat Neurosci 3:1098-1106.

Ziburkus J, Dilger Ek, Lo FS, Guido W (2009) LTD and LTP at the developing retinogeniculate synapse. J Neurophysiol 102:3082-3090.

Ziburkus J, Guido W (2006) Loss of binocular responses and reduced retinal convergence during the period of retinogeniculate axon segregation. J Neurophysiol 96:2775-2784.

Ziburkus J, Lo FS, Guido W (2003) Nature of inhibitory postsynaptic activity in developing relay cells of the lateral geniculate nucleus. J Neurophysiol 90:1063-1070.

Publishing Agreement

It is the policy of the University to encourage the distribution of all theses, dissertations, and manuscripts. Copies of all UCSF theses, dissertations, and manuscripts will be routed to the library via the Graduate Division. The library will make all theses, dissertations, and manuscripts accessible to the public and will preserve these to the best of their abilities, in perpetuity.

Please sign the following statement:

I hereby grant permission to the Graduate Division of the University of California, San Francisco to release copies of my thesis, dissertation, or manuscript to the Campus Library to provide access and preservation, in whole or in part, in perpetuity.

Selena Koch
Author Signature

6/7/2011
Date